

# Hydrodynamics of a hard-core non-polar active lattice gas

Ritwik Mukherjee,<sup>1,\*</sup> Soumyabrata Saha,<sup>2,†</sup> Tridib Sadhu,<sup>2,‡</sup> Abhishek Dhar,<sup>1,§</sup> and Sanjib Sabhapandit<sup>3,¶</sup>

<sup>1</sup>International Centre for Theoretical Sciences, Tata Institute of Fundamental Research, Bangalore 560089, India

<sup>2</sup>Department of Theoretical Physics, Tata Institute of Fundamental Research, Mumbai 400005, India

<sup>3</sup>Raman Research Institute, Bangalore 560080, India

We present a fluctuating hydrodynamic description of a non-polar active lattice gas model with excluded volume interactions that exhibits motility-induced phase separation under appropriate conditions. For quasi-one dimension and higher, stability analysis of the noiseless hydrodynamics gives quantitative bounds on the phase boundary of the motility-induced phase separation in terms of spinodal and binodal. Inclusion of the multiplicative noise in the fluctuating hydrodynamics describes the exponentially decaying two-point correlations in the stationary-state homogeneous phase. Our hydrodynamic description and theoretical predictions based on it are in excellent agreement with our Monte-Carlo simulations and pseudo-spectral iteration of the hydrodynamics equations. Our construction of hydrodynamics for this model is not suitable in strictly one-dimension with single-file constraints, and we argue that this breakdown is associated with micro-phase separation.

Active matter commonly refers to non-equilibrium systems with energy injections at the microscopic scale that independently drives individual constituents and often leads to large scale self-organized structures [1–4]. Although they are inspired by living matter, active systems have been realized in synthetic objects like Janus particles [5], vibrated rods [6], driven granular systems [7], motor driven robots [8, 9], and even in quantum matter [10]. The prominence of the field comes from the novel emergent collective behaviours that often comes as a surprise from an equilibrium viewpoint. Beside their potential applicability [11, 12], these emergent many-body structures poses an intriguing challenge for non-equilibrium statistical mechanics. In recent decades, major efforts have been devoted in developing a theoretical understanding based on effective field theories [13] and large scale computer simulations [14–16]. However, even for simple characteristic many-body phases of active matter, namely the Motility-Induced Phase Separation (MIPS) [17, 18], there is no clear bottom-up theoretical understanding, analogous to equilibrium statistical mechanics for liquid-gas coexistence, that could relate the large scale phases to the underlying microscopic dynamics.

A promising bottom-up approach for many-body dynamics is in terms of fluctuating hydrodynamics, that has been phenomenally successful in capturing non-equilibrium fluctuations in diffusive transport models [19], Hamiltonian dynamical systems [20, 21], and even in quantum integrable models [22–24]. Hydrodynamics description has also proven tremendously effective in active matter [25, 26], although a rigorous derivation relating to microscopic dynamics is available only for a handful of cases. One such example is an active lattice gas [27], whose hydrodynamics was proven in mathematical terms and its fluctuation-extension incorporating a stochasticity has been recently obtained [28, 29] using intriguing mapping to a well-known exclusion process. However, the model involves an exchange dynamics between particles that seems unphysical, presumably incorporated to sustain MIPS. Most well-known off-lattice active dynamics [17, 30–32] are for impassable particles with finite volume hard-core which provides the much-needed activity induced caging effect to

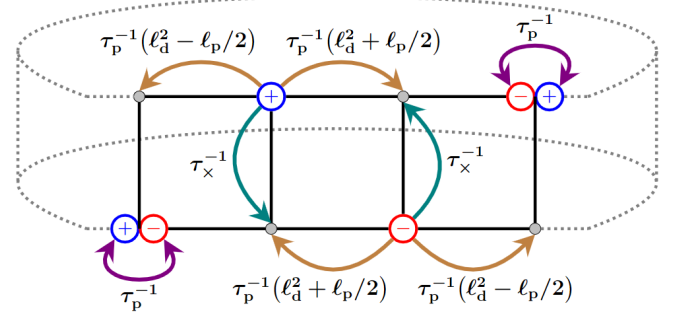


FIG. 1. **Model:** A schematic of the model defined in 1-3, on a two-lane ladder-lattice with periodic boundary condition.

sustain MIPS. In fact, volume exclusion is expected in natural examples of living or synthetic active matter.

In this *Letter*, we propose a lattice model, that is inspired by [27], but without the exchange dynamics. The dynamics of our model is closer to realistic off-lattice dynamics of non-polar active matter that are known to exhibit MIPS [17]. For our model in the quasi-one dimension of a periodic two-lane ladder-lattice (see Fig. 1), there is a stable MIPS state at certain range of high activity and density. For this model, we derive the fluctuating hydrodynamics using a field-theoretical approach that is generalizable and independent of the previous method in [28, 29]. Within the hydrodynamics we show how dynamical instabilities of the coupled equations of hydrodynamic fields quantitatively bound the MIPS boundaries (see Fig. 3). Moreover, we find that correlations from the fluctuating hydrodynamics have excellent agreement with their Monte-Carlo results and captures the qualitative features seen [33] in well-known off-lattice active matter models. Our construction of the hydrodynamics straightforwardly extends for the higher dimensional generalization of the model and in particular, they capture the existence of MIPS in two dimensions.

For strictly one-dimensional periodic lattice, our hydrodynamics construction predicts MIPS which is however not observed in our Monte-Carlo simulation. This indicates that

our specific hydrodynamics construction is not suitable in one-dimension with a single-file constraint, resonating similar findings [34, 35]. We argue that this discrepancy has a subtle origin on the formation of micro-clusters.

*A quasi-1D model* — We consider a two-species lattice-gas with average density  $\rho_0 \in [0, 1]$ , on a periodic two-lane ladder-lattice (see Fig. 1), with each lane  $j = \{1, 2\}$  containing  $L$  sites indexed as  $i = \{1, 2, \dots, L\}$ . To incorporate hard-core repulsion among particles, we enforce a simple exclusion condition that each site can contain at most one particle at a given instance. The two species denoted by (+) and (−), representing internal orientations of an active particle, follow a persistent dynamics on the lattice with intermittent switching of the orientations, as defined below.

1. Biased diffusion: a (+) particle at site  $(i, j)$  hops to site  $(i \pm 1, j)$  at rate  $\tau_p^{-1} [(\ell_d/a)^2 \pm (\ell_p/a)/2]$  while a (−) particle at site  $(i, j)$  hops to  $(i \pm 1, j)$  site at rate  $\tau_p^{-1} [(\ell_d/a)^2 \mp (\ell_p/a)/2]$ , provided the target site is empty.
2. Tumbling: a (+) particle at any site converts to a (−) particle at rate  $\tau_p^{-1}$  and vice versa.
3. Lane-crossing: a particle at a site  $(i, 1)$  on lane-1 hops to the site  $(i, 2)$  on lane-2 at rate  $\tau_x^{-1}$  and vice versa, provided the target site is empty.

The above dynamics mimics self-propelled particles with persistence-time  $\tau_p$ , self-propulsion speed  $\ell_p/\tau_p$ , and thermal-diffusivity  $D = \ell_d^2/\tau_p$ . The internal state ( $\pm$ ) represents particle's preferred direction of motion, towards right and left, respectively. The ratio of the persistent length  $\ell_p$  and the diffusive length  $\ell_d$ , known as the Péclet number  $Pe = \ell_p/\ell_d$ , is a standard measure of activity. The parameter  $a$  denotes lattice spacing, which we set to unity throughout this Letter.

The quasi-one dimensional geometry with the lane crossing effectively describes motion inside narrow channels, where particle size is comparable to the diameter of the channel, allowing occasional crossing [36–39], but at a much reduced rate compared to the exchange rate in [27], resulting in a different hydrodynamics.

A microscopic configuration of the system at a given time  $\tau$  is specified in terms of the binary occupation variables  $n_{i,j}^\pm(\tau)$  for each species  $\sigma = (\pm)$  respectively, where  $n_{i,j}^\sigma(\tau) = 1$  or 0 depending on whether the site  $(i, j)$  is occupied by the species  $\sigma$  or not. A more convenient choice to describe the dynamics is in terms of the total occupation variable,  $n_{i,j} = n_{i,j}^+ + n_{i,j}^-$  and the polarization variable,  $M_{i,j} = n_{i,j}^+ - n_{i,j}^-$ . Due to the exclusion condition,  $n_{i,j} = \{0, 1\}$  depending on the occupancy of the site, while  $M_{i,j} = \{0, \pm 1\}$  depending on the species of the occupant.

We now present a hydrodynamic description by coarse-graining these variables such that fast fluctuations are locally equilibrated over a hydrodynamic scale and slow modes smoothly evolve. For our dynamics the relevant length and time scales are  $\ell_d$  and  $\tau_p$ . The hydrodynamics is defined in the re-scaled coordinates  $(x, t) := (i/\ell_d, \tau/\tau_p)$ , by taking  $\ell_d, \ell_p$  and  $\tau_p$  large, while keeping the diffusivity  $D = \ell_d^2/\tau_p$  and the Péclet number  $Pe = \ell_p/\ell_d$  finite. For finite  $\tau_x \ll \tau_p$ ,

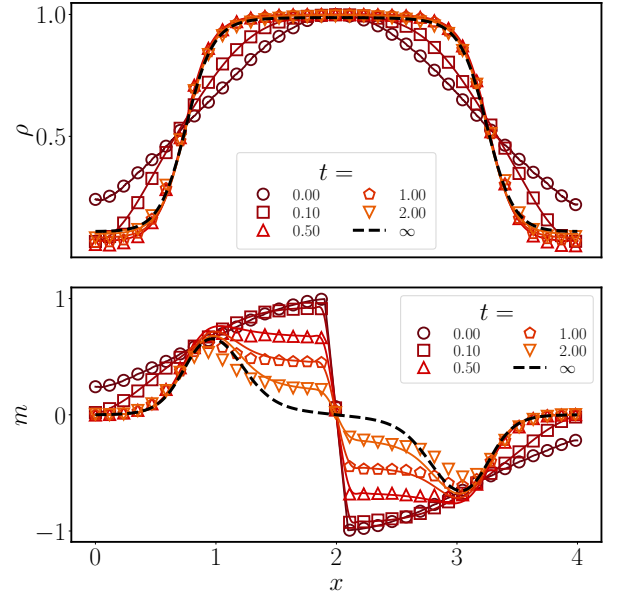


FIG. 2. **Test of hydrodynamics:** Time evolution of the hydrodynamic density  $\rho(x, t)$  and polarization  $m(x, t)$ , starting from a Gaussian profile  $\rho(x, 0)$  centered around the middle of the system, with (+) particles placed at the left-half and (−) particles at the right-half. The solid lines represent noiseless hydrodynamic evolution (1), while the points represent Monte-Carlo simulations of the microscopic dynamics in 1-3. The dashed lines indicate the steady state profile from hydrodynamics. The plots are for microscopic parameter values  $\ell_d = 1024$ ,  $\tau_p = 2.5\ell_d^2$ ,  $\ell_p = 10\ell_d$ ,  $\tau_x = 0.1$  and system size  $L = 4\ell_d$ , which corresponds to  $Pe = 10$ .

the adjacent sites of the two lanes effectively equilibrates at the hydrodynamic scale, implying their evolution is described by the same coarse-grained variables  $n_{i,j}(\tau) \simeq \rho(x, t)$  and  $M_{i,j}(\tau) \simeq m(x, t)$ , independent of the lane-index  $j$ .

We show [40] that the evolution of  $\rho(x, t)$  and  $m(x, t)$  follows the coupled fluctuating hydrodynamics

$$\partial_t \rho = \partial_x^2 \rho - Pe \partial_x [m(1 - \rho)] + \ell_d^{-1/2} \partial_x \eta_p \quad (1a)$$

$$\begin{aligned} \partial_t m = & (1 - \rho) \partial_x^2 m + m \partial_x^2 \rho - Pe \partial_x [\rho(1 - \rho)] - 2m \\ & + \ell_d^{-1/2} (\partial_x \eta_m + 2\eta_f), \end{aligned} \quad (1b)$$

where  $\eta_p$ ,  $\eta_m$  and  $\eta_f$  are Gaussian noises each of zero mean with covariance  $\langle \eta_p(x, t) \eta_q(x', t') \rangle = S_{p,q} \delta(x - x') \delta(t - t')$ , with the mobility matrix  $S_{p,p} = S_{m,m} = 2\rho(1 - \rho)$ ,  $S_{p,m} = S_{m,p} = 2m(1 - \rho)$ ,  $S_{f,f} = \rho$ , and zero for the rest. The non-conservative noise  $\eta_f$  is due to tumbling events in the dynamics. The same hydrodynamics extends for multi-lane generalizations with the number of lanes  $\ll \ell_d$ .

Our detailed derivation for (1), presented in the Supplemental Materials (SM) [40], is based on an evaluation of the Martin-Siggia-Rose-Janssen-de Dominicis action of the stochastic differential equation (1) following a coarse-graining of the microscopic generator [41]. This method is generalizable for variations of the dynamics and dimension-

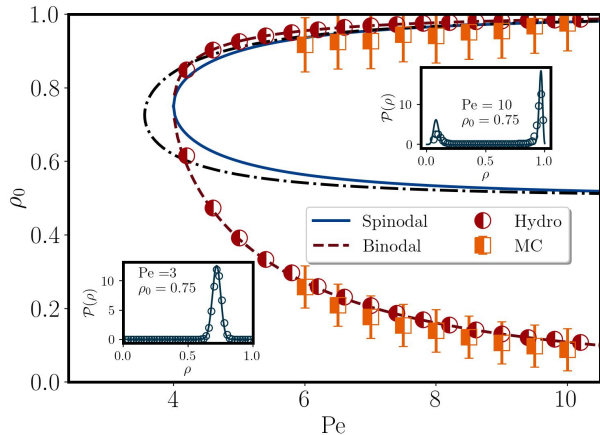


FIG. 3. **Phase Diagram:** Spinodal and binodal, given by (2) and (3) respectively, plotted with the solid and dashed lines. Along the dash-dotted line, the pre-factor of the exponential in (4) diverges. The points represent the ‘liquid’ and ‘gas’ densities obtained from Monte-Carlo simulations and numerical iteration of hydrodynamics. The error bars indicate the uncertainty due to the width of the density distribution around the peaks shown in the insets. The bimodal density distribution inside the spinodal region is an indication of MIPS, whereas the unimodal density distribution outside the binodal region is an indication of the homogeneous phase. In the inset, the points are from Monte-Carlo simulations and the solid lines are from an analytical calculation [40]. We use  $L = 4096$  in Monte-Carlo simulations and hydrodynamics equation solved numerically using Fourier spectral method with 1024 modes.

ality. It is fundamentally different from a derivation [28] for a related model [27], which rests on mapping to stochastic diffusive models whose hydrodynamics is well-tested. Such mapping relies on a very specific choice of the parameters, and not extendable for our model. Compared to the hydrodynamics in [27, 28], the diffusion matrix and the mobility matrix are significantly different.

In Fig. 2 we compare the noiseless hydrodynamics, setting all the Gaussian noises in (1) to zero, with direct Monte-Carlo simulation of the microscopic dynamics 1-3. In the initial state, the left half of the system is occupied with (+) particles and the right half with (-) particles, each drawn from a Bernoulli distribution with a site-dependent average density,  $\langle n_i \rangle = \rho(i/\ell_d, 0)$ , set in Fig. 2 such that bulk density  $\rho_0 = (\ell_d/L) \int \rho(x, 0) dx = 0.66$ . We convert the microscopic occupation profile to the hydrodynamic density and polarization profile by coarse-graining over boxes containing 200 sites. Only profiles of one lane, averaged over 64 ensembles, are shown in Fig. 2 as the two lanes locally equilibrate at hydrodynamic times  $\tau_x/\tau_p \sim 10^{-7}$ . For iterating the noiseless hydrodynamics we numerically integrate (1) without the noise terms using a Fourier-pseudospectral method [42], treating nonlinear terms in real space and linear terms in Fourier space with  $2^{10}$  modes. An excellent agreement seen in the evolution of the profiles, asymptotically converging towards an inhomogeneous state, indicates a phase separation between

high density and low-density regions.

It is readily seen from (1) that uniform density  $\rho(x) = \rho_0$  and  $m(x) = 0$  is a stationary solution of the noiseless hydrodynamics. An inhomogeneous phase-separated state, widely known as the MIPS for active matter systems, is an indication of the instability of this globally homogeneous solution. The spinodal curve on the  $(Pe, \rho_0)$  plane describes the onset of instability against linear perturbations. A standard linear stability analysis [40] of the noiseless hydrodynamics (1) predicts  $Pe^2(1 - \rho_0)(2\rho_0 - 1) > 2$  as the unstable regimes. Thus, for  $0 < Pe < 4$ , a homogeneous state with any density  $0 < \rho_0 < 1$  is always stable under linear perturbations. On the other hand, for  $Pe > 4$ , the homogeneous state is unstable if

$$\frac{3}{4} - \frac{1}{4} \sqrt{1 - \left(\frac{4}{Pe}\right)^2} < \rho_0 < \frac{3}{4} + \frac{1}{4} \sqrt{1 - \left(\frac{4}{Pe}\right)^2}. \quad (2)$$

The spinodal curve is shown in Fig. 3. Indeed, we see from Fig. 2 that if the parameters  $(Pe, \rho_0)$  are chosen from within the spinodal region, the density profile  $\rho(x, t)$  evolves to an inhomogeneous state. The spinodal region given by Eq. (2) incidentally coincides with that for the model in [27].

The binodal curve gives the two densities in a phase-separated state where a “liquid-like” high-density  $\rho_l$  phase coexists with a “gas-like” low-density  $\rho_g$  phase. Following [43, 44], we find that [40] for our noiseless hydrodynamics (1), the two coexistence densities are determined by a pair of relations

$$g_0(\rho_g) = g_0(\rho_l) \quad \text{and} \quad h_0(\rho_g) = h_0(\rho_l), \quad (3)$$

where  $g_0(\rho) = Pe\rho(1 - \rho) - (2/Pe)\log(1 - \rho)$  and  $h_0(\rho) = [2/(9Pe)](1 - \rho)^{-3} + (Pe/6)(3 - 4\rho)(1 - \rho)^{-2}$ . We numerically solve the above pair of relations (3) and obtain the binodal curve, which we plot in Fig. 3 along with the spinodal. Evidently, the volume fraction  $\phi$  of the “liquid” region(s) is given by  $\rho_l\phi + \rho_g(1 - \phi) = \rho_0$ , i.e.,  $\phi = (\rho_0 - \rho_g)/(\rho_l - \rho_g)$ . Therefore, for  $Pe > 4$ , for any global density  $\rho_g < \rho_0 < \rho_l$ , it is possible to sustain a nonzero fraction  $0 < \phi < 1$  of a liquid region within the analysis of the noiseless hydrodynamics. In particular, the parameters between the spinodal and the binodal curves correspond to a metastable region where, depending on the initial condition, the noiseless hydrodynamics (1) leads to either a homogeneous state or a phase-separated state [40].

We also numerically iterate the noiseless hydrodynamics (1) for a long time so that it reaches a stationary state, and determine the steady state ‘liquid’ and ‘gas’ densities, by choosing the minimum and maximum densities in the density profile, respectively. However, in Monte-Carlo simulations, identifying the lowest and highest densities is less straightforward due to the fluctuating nature of the density profile. To address this, we extract density distributions and average them over steady-state profiles (depicted in the inset). The resulting bimodal density distribution indicates the presence of two distinct densities, characteristic of MIPS.



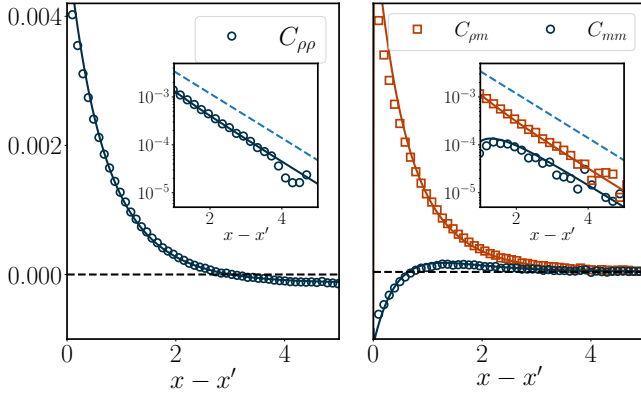


FIG. 4. **Correlations:** Solid lines plot the analytical results of the correlation functions whereas the points are from numerical simulations. The insets show the asymptotic decay of the correlation functions (with a constant shift in order to show up in the log-linear plot), with the dashed guiding lines plot (4) with a shift for better visibility. The parameters used in the simulations are  $\ell_d = 10.24$ ,  $\tau_p = 2\ell_d^2$ ,  $\ell_p = 2\ell_d$ ,  $\tau_x = 0.1$ ,  $L = 100\ell_d$  and  $\rho_0 = 0.25$ , and we average over  $10^5$  statistically-independent time steps to generate a clean curve for comparing with hydrodynamic predictions.

We now compute the correlation functions in the stationary-state homogeneous phase, using fluctuating hydrodynamics of (1). For example, The density-density correlations for far-separated points in the stationary-state homogeneous phase has the asymptote [40]

$$C_{\rho\rho}(x, x') \simeq \frac{A}{B\ell_d} \exp\left(-\frac{|x-x'|}{\xi_1}\right) \quad (4)$$

where  $A = \text{Pe}^2 \rho_0^2 (1 - \rho_0)^2 / \sqrt{1 - \rho_0/2}$ ,  $B = 2 - \text{Pe}^2 (1 - \rho_0)(2 - \rho_0)(2\rho_0 - 1)$ , and the correlation length  $\xi_1 = \sqrt{1 - \rho_0/2}$ . The line along which the denominator  $B$  vanishes, indicating breakdown of linearized hydrodynamics, is shown in Fig. 3. Its full form and the other correlation functions are given in SM [40]. We compare our analytical correlation predictions with Monte-Carlo simulations in Fig. 4 and find excellent agreements. An indirect verification of the multiplicative noise terms in (1) comes from this comparison of correlations with Monte-Carlo results.

*Generalization to  $d$ -dimensions* — There are several ways one can generalize our quasi-1D model to higher dimensions. The straightforward generalization takes the number of lanes to be  $O(\ell_d)$  with  $\tau_x = \ell_d^2 / \tau_p$ . In this case, the noiseless hydrodynamic description along the *active* direction remains the same [40] as in the quasi-1D case. On the other hand, in an isotropic generalization, we define the  $d$ -dimensional version of the model on a periodic hyper-cubic lattice of  $L^d$  sites and average density  $\rho_0 \in [0, 1]$ . The lattice sites indexed as  $(i_1, i_2, \dots, i_d)$ , where  $i_k = 1, 2, \dots, L$  with  $k = 1, 2, \dots, d$ . The system is composed of  $2d$  distinct species denoted by  $\sigma = 1, 2, \dots, 2d$  corresponding to the  $2d$  possible directions of self-propulsion denoted by  $\hat{r}_\sigma = \pm\hat{x}_1, \pm\hat{x}_2, \dots, \pm\hat{x}_d$ . In this model, a particle of  $\sigma$ -species hops at rate  $\tau_p^{-1}(\ell_d^2 + \ell_p/2)$  in

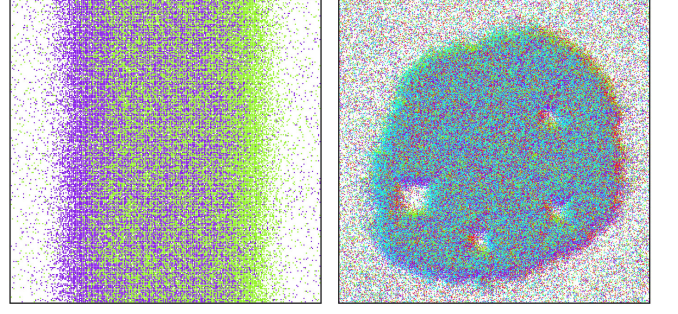


FIG. 5. **MIPS:** Monte-Carlo simulation for the two-dimensional models on a  $512 \times 512$  square lattice with  $\rho_0 = 0.62$ . Left figure corresponds to the 2-species ( $\rightarrow$  and  $\leftarrow$ ) generalization and right to the 4-species ( $\rightarrow$ ,  $\uparrow$ ,  $\leftarrow$  and  $\downarrow$ ) generalization. The colors indicate species (magenta  $\equiv \rightarrow$ , cyan  $\equiv \uparrow$ , green  $\equiv \leftarrow$ , red  $\equiv \downarrow$ ). For the 2-species model  $\ell_d = 128$  and for the 4-species model  $\ell_d = 32$ , with  $\text{Pe} = 12$  and  $\tau_p = \ell_d^2$  in both cases.

the  $\hat{r}_\sigma$ -direction and at rate  $\tau_p^{-1}(\ell_d^2 - \ell_p/2)$  in the other  $2d - 1$  directions, provided that the target site is empty. In addition, a particle changes its species, i.e. tumbles, at rate  $\tau_p^{-1}$ . The fluctuating hydrodynamics for this microscopic dynamics turns out to be [40]

$$\begin{aligned} \partial_t \rho_\sigma &= (1 - \rho) \nabla^2 \rho_\sigma + \rho_\sigma \nabla^2 \rho - \text{Pe} \vec{\nabla} [\rho_\sigma (1 - \rho)] \cdot \hat{r}_\sigma \\ &\quad - \sum_{\sigma' \neq \sigma} (\rho_\sigma - \rho_{\sigma'}) + \ell_d^{-d/2} \left[ \vec{\nabla} \cdot \vec{\eta}_\sigma + \sum_{\sigma' \neq \sigma} \eta_{\sigma \rightarrow \sigma'} \right] \end{aligned} \quad (5)$$

Here, the conservative zero-mean Gaussian noise,  $\vec{\eta}_\sigma = (\eta_\sigma^{(1)}, \eta_\sigma^{(2)}, \dots, \eta_\sigma^{(d)})$  arising from the biased-hopping dynamics, has the covariance  $\langle \eta_\sigma^{(k)}(\vec{x}, t) \eta_{\sigma'}^{(k')}(\vec{x}', t') \rangle = 2\rho_\sigma (1 - \rho) \delta_{\sigma, \sigma'} \delta_{k, k'} \delta(\vec{x} - \vec{x}') \delta(t - t')$  while the non-conservative zero mean Gaussian noise,  $\eta_{\sigma \rightarrow \sigma'} = -\eta_{\sigma' \rightarrow \sigma}$ , arising from the tumbling dynamics, has the covariance  $\langle \eta_{\sigma \rightarrow \sigma'}(\vec{x}, t) \eta_{\psi \rightarrow \psi'}(\vec{x}', t') \rangle = (\rho_\sigma + \rho_{\sigma'}) \delta_{\sigma, \psi} \delta_{\sigma', \psi'} \delta(\vec{x} - \vec{x}') \delta(t - t')$ .

Since the analysis of the above hydrodynamics equation (5) is similar to the quasi-1D case, we do not repeat it here. Instead, we perform Monte-Carlo simulations for the two-dimensional microscopic model ( $d = 2$ ) with both generalizations. We observe MIPS in our simulations for some parameters, as shown in Fig. 5, indicating that MIPS can emerge in 2D systems, even without the exchange dynamics of [27]. Therefore, in dimensions higher than one, neither achieving a strong mixing effect nor observing the MIPS requires an exchange dynamics between the particles making our choice of dynamics naturally conducive for the desired results.

*A strictly 1D model* — For the version of our model on a periodic one-lane lattice with the dynamics 1-2, exclusion interaction introduces single-file constraint, which preserves positional order of the particles. Our hydrodynamics construction, relying on an assumption of local equilibrium measure, predicts the same fluctuating hydrodynamics (1) as in the quasi-1D case, which predicts the same phase boundary as in Fig. 3. However, our Monte-Carlo simulation of this 1D

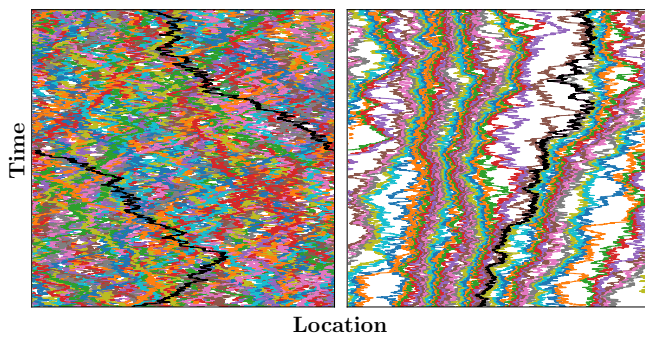


FIG. 6. **Kymographs:** Comparison of space-time trajectories of particles at long hydrodynamic times for two-lane (left) and one-lane (right) models. The black color indicates a tracer. The figures correspond to parameter values ( $Pe = 6$ , and  $\rho_0 = 0.2$ ) outside the binodal curve in Fig. 3.

model does not support MIPS [45] for the parameter ranges in Fig. 3. Evidently, the predicted hydrodynamics does not work for this strictly 1D geometry. This is further confirmed by a direct comparison of the noiseless evolution (1) of average fields with Monte-Carlo simulation [40].

A hydrodynamics is by construction about effective dynamics of slow modes rising from local equilibrium of fast modes. Compared to higher dimensions, the single-file constraint in 1D preserves the local order of species, and therefore, local polarization at microscopic time scales  $\ll \tau_p$ . This fight between activity and local conservation, results in formation of large number of micro-clusters, that does not coarsen as seen in the Kymographs of particles in Fig. 6. Compared to the fluid-like evolution in the two-lane model in its homogeneous phase, the particle movements are severely restricted in the one-lane model at the same parameter values. This reduced effective diffusivity and drift of particles break [40] our specific assumption about local equilibration, invalidating the hydrodynamics construction.

**Conclusion** — In the spirit of statistical mechanics, we have proposed a minimal model of interacting non-polar active particles where simplest kind of steric interaction leads to macroscopic phase separation, which is a well-known consequence of activity. Simplicity of the model allows us to theoretically analyse the macroscopic properties using a systematic bottom-up hydrodynamics theory. This hydrodynamic formulation potentially could serve as a minimal macroscopic description for MIPS, that is shared between different microscopic models, in the spirit of the Landau theory of phase transitions. There is a plethora of active dynamics [15, 30, 46, 47] belonging to this class for which a detailed fluctuating hydrodynamics is not available. It would be interesting to see how much of the fluctuating hydrodynamics results for the present work compares in other models, including a full characterization of macroscopic fluctuations in terms of large deviations [48–51]. Our current work paves a crucial step in this promising direction.

**Acknowledgments:** We thank S Jose, J U Klamser, S

Mukherjee, S Paul, K Ramola, S S Ray, and J C Sunil for stimulating discussions. AD and TS acknowledge financial support of the Department of Atomic Energy, Government of India, under Project Identification No. RTI 4001 and RTI 4002. AD acknowledges the J.C. Bose Fellowship (JCB/2022/000014) of the Science and Engineering Research Board of the Department of Science and Technology, Government of India. This research was supported in part by the International Centre for Theoretical Sciences (ICTS) for participating in the program - Statistical Physics of Complex Systems (code: ICTS/SPCS2022/12) and the 9th Indian Statistical Physics Community Meeting (code: ICTS/ISPCM2024/4).

\* [ritwik.mukherjee@icts.res.in](mailto:ritwik.mukherjee@icts.res.in)

† [soumyabrata.saha@tifr.res.in](mailto:soumyabrata.saha@tifr.res.in)

‡ [tridib@theory.tifr.res.in](mailto:tridib@theory.tifr.res.in)

§ [abhishek.dhar@icts.res.in](mailto:abhishek.dhar@icts.res.in)

¶ [sanjib@rri.res.in](mailto:sanjib@rri.res.in)

- [1] M. J. Bowick, N. Fakhri, M. C. Marchetti, and S. Ramaswamy, Symmetry, thermodynamics, and topology in active matter, *Phys. Rev. X* **12**, 010501 (2022).
- [2] S. Ramaswamy, Active matter, *J. Stat. Mech.* **2017**, 054002 (2017).
- [3] S. Ramaswamy, The mechanics and statistics of active matter, *Annu. Rev. Condens. Matter Phys.* **1**, 323–345 (2010).
- [4] M. C. Marchetti, J. F. Joanny, S. Ramaswamy, T. B. Liverpool, J. Prost, M. Rao, and R. A. Simha, Hydrodynamics of soft active matter, *Rev. Mod. Phys.* **85**, 1143 (2013).
- [5] T. Vicsek, A. Czirók, E. Ben-Jacob, I. Cohen, and O. Shochet, Novel type of phase transition in a system of self-driven particles, *Phys. Rev. Lett.* **75**, 1226 (1995).
- [6] J. Deseigne, S. Léonard, O. Dauchot, and H. Chaté, Vibrated polar disks: Spontaneous motion, binary collisions, and collective dynamics, *Soft Matter* **8**, 5629–5639 (2012).
- [7] J. Deseigne, O. Dauchot, and H. Chaté, Collective motion of vibrated polar disks, *Phys. Rev. Lett.* **105**, 098001 (2010).
- [8] G. Wang, T. V. Phan, S. Li, M. Wombacher, J. Qu, Y. Peng, G. Chen, D. I. Goldman, S. A. Levin, R. H. Austin, and L. Liu, Emergent field-driven robot swarm states, *Phys. Rev. Lett.* **126**, 108002 (2021).
- [9] V. A. Webster-Wood, M. Guix, N. W. Xu, B. Behkam, H. Sato, D. Sarkar, S. Sanchez, M. Shimizu, and K. K. Parker, Biohybrid robots: Recent progress, challenges, and perspectives, *Bioinspir. Biomim.* **18**, 015001 (2022).
- [10] R. Khasseh, S. Wald, R. Moessner, C. A. Weber, and M. Heyl, Active quantum flocks (2023), [arXiv:2308.01603 \[quant-ph\]](https://arxiv.org/abs/2308.01603).
- [11] G. Frangipane, D. Dell’Arciprete, S. Petracchini, C. Maggi, F. Saglimbeni, S. Bianchi, G. Vizsnyiczai, M. L. Bernardini, and R. Di Leonardo, Dynamic density shaping of photokinetic *E. coli*, *eLife* **7**, e36608 (2018).
- [12] É. Fodor and M. E. Cates, Active engines thermodynamics moves forward, *EPL* **134**, 10003 (2021).
- [13] M. E. Cates, Active field theories, in *Active Matter and Nonequilibrium Statistical Physics: Lecture Notes of the Les Houches Summer School: Volume 112, September 2018* (Oxford University Press, 2022) Chap. 6, p. 180–216.
- [14] M. R. Shaebani, A. Wysocki, R. G. Winkler, G. Gompper, and H. Rieger, Computational models for active matter, *Nat. Rev.*

- Phys.* **2**, 181–199 (2020).
- [15] J. U. Klamser, O. Dauchot, and J. Tailleur, Kinetic Monte Carlo algorithms for active matter systems, *Phys. Rev. Lett.* **127**, 150602 (2021).
- [16] B. Sabass, R. G. Winkler, T. Auth, J. Elgeti, D. A. Fedosov, M. Ripoll, G. A. Vliegenthart, and G. Gompper, Computational physics of active matter, in *Out-of-equilibrium Soft Matter* (The Royal Society of Chemistry, 2023) Chap. 10, p. 354–390.
- [17] M. E. Cates and J. Tailleur, Motility-induced phase separation, *Annu. Rev. Condens. Matter Phys.* **6**, 219–244 (2015).
- [18] J. O’Byrne, A. Solon, J. Tailleur, and Y. Zhao, An introduction to motility-induced phase separation, in *Out-of-equilibrium Soft Matter* (The Royal Society of Chemistry, 2023) Chap. 4, p. 107–150.
- [19] L. Bertini, A. De Sole, D. Gabrielli, G. Jona-Lasinio, and C. Landim, Macroscopic fluctuation theory, *Rev. Mod. Phys.* **87**, 593 (2015).
- [20] B. Doyon, Exact large-scale correlations in integrable systems out of equilibrium, *SciPost Phys.* **5**, 054 (2018).
- [21] H. Spohn, Nonlinear fluctuating hydrodynamics for anharmonic chains, *J. Stat. Phys.* **154**, 1191–1227 (2014).
- [22] B. Bertini, M. Collura, J. De Nardis, and M. Fagotti, Transport in out-of-equilibrium XXZ chains: Exact profiles of charges and currents, *Phys. Rev. Lett.* **117**, 207201 (2016).
- [23] O. A. Castro-Alvaredo, B. Doyon, and T. Yoshimura, Emergent hydrodynamics in integrable quantum systems out of equilibrium, *Phys. Rev. X* **6**, 041065 (2016).
- [24] J. De Nardis, D. Bernard, and B. Doyon, Hydrodynamic diffusion in integrable systems, *Phys. Rev. Lett.* **121**, 160603 (2018).
- [25] R. A. Simha and S. Ramaswamy, Hydrodynamic fluctuations and instabilities in ordered suspensions of self-propelled particles, *Phys. Rev. Lett.* **89**, 058101 (2002).
- [26] J. Toner, Y. Tu, and S. Ramaswamy, Hydrodynamics and phases of flocks, *Ann. Phys.* **318**, 170–244 (2005).
- [27] M. Kourbane-Houssene, C. Erignoux, T. Bodineau, and J. Tailleur, Exact hydrodynamic description of active lattice gases, *Phys. Rev. Lett.* **120**, 268003 (2018).
- [28] T. Agranov, S. Ro, Y. Kafri, and V. Lecomte, Exact fluctuating hydrodynamics of active lattice gases — typical fluctuations, *J. Stat. Mech.* **2021**, 083208 (2021).
- [29] T. Agranov, S. Ro, Y. Kafri, and V. Lecomte, Macroscopic fluctuation theory and current fluctuations in active lattice gases, *SciPost Phys.* **14**, 045 (2023).
- [30] P. Digregorio, D. Levis, A. Suma, L. F. Cugliandolo, G. Gonnella, and I. Pagonabarraga, Full phase diagram of active Brownian disks: From melting to motility-induced phase separation, *Phys. Rev. Lett.* **121**, 098003 (2018).
- [31] J. U. Klamser, S. C. Kapfer, and W. W. Krauth, Thermodynamic phases in two-dimensional active matter, *Nature Communications* **9**, 5045 (2018).
- [32] F. Caballero, C. Nardini, and M. E. Cates, From bulk to microphase separation in scalar active matter: a perturbative renormalization group analysis, *J. Stat. Mech.* **2018**, 123208 (2018).
- [33] G. Szamel and E. Flenner, Long-ranged velocity correlations in dense systems of self-propelled particles, *EPL* **133**, 60002 (2021).
- [34] O. Blondel, C. Erignoux, and M. Simon, Stefan problem for a nonergodic facilitated exclusion process, *Probab. Math. Phys.* **2**, 127–178 (2021).
- [35] L. Touzo, P. Le Doussal, and G. Schehr, Interacting, running and tumbling: The active Dyson Brownian motion, *EPL* **142**, 61004 (2023).
- [36] U. Siems, C. Kreuter, A. Erbe, N. Schwierz, S. Sengupta, P. Leiderer, and P. Nielaba, Non-monotonic crossover from single-file to regular diffusion in micro-channels, *Sci. Rep.* **2**, 1015 (2012).
- [37] A. Miron, D. Mukamel, and H. A. Posch, Phase transition in a 1d driven tracer model, *J. Stat. Mech.* **2020**, 063216 (2020).
- [38] P. Wilke, E. Reithmann, and E. Frey, Two-species active transport along cylindrical biofilaments is limited by emergent topological hindrance, *Phys Rev X* **8**, 031063 (2018).
- [39] R. Nandi, U. C. Täuber, and Priyanka, Dynein-inspired multi-lane exclusion process with open boundary conditions, *Entropy* **23**, 1343 (2021).
- [40] See Supplemental Materials for details.
- [41] S. Saha and T. Sadhu, Large deviations in the symmetric simple exclusion process with slow boundaries: A hydrodynamic perspective (2023), [arXiv:2310.11350v2 \[cond-mat.stat-mech\]](https://arxiv.org/abs/2310.11350v2).
- [42] L. N. Trefethen, *Spectral methods in MATLAB* (SIAM Philadelphia, 2000).
- [43] A. P. Solon, J. Stenhammar, M. E. Cates, Y. Kafri, and J. Tailleur, Generalized thermodynamics of phase equilibria in scalar active matter, *Phys. Rev. E* **97**, 020602(R) (2018).
- [44] A. P. Solon, J. Stenhammar, M. E. Cates, Y. Kafri, and J. Tailleur, Generalized thermodynamics of motility-induced phase separation: phase equilibria, laplace pressure, and change of ensembles, *New J. Phys.* **20**, 075001 (2018).
- [45] I. Mukherjee, A. Raghu, and P. K. Mohanty, Nonexistence of motility induced phase separation transition in one dimension, *SciPost Phys.* **14**, 165 (2023).
- [46] Y-E Keta, R. L. Jack, and L. Berthier, Disordered collective motion in dense assemblies of persistent particles, *Phys. Rev. Lett.* **129**, 048002 (2022).
- [47] J. Mason, C. Erignoux, R. L. Jack, and M. Bruna, Exact hydrodynamics and onset of phase separation for an active exclusion process, *Proc. R. Soc. A* **479**, 20230524 (2023).
- [48] T. Bodineau and B. Derrida, Distribution of current in nonequilibrium diffusive systems and phase transitions, *Phys. Rev. E* **72**, 066110 (2005).
- [49] G. Bunin, Y. Kafri, and D. Podolsky, Non-differentiable large-deviation functionals in boundary-driven diffusive systems, *J. Stat. Mech.* **2012**, L10001 (2012).
- [50] P. Tsobgni Nyawo and H. Touchette, Large deviations of the current for driven periodic diffusions, *Phys. Rev. E* **94**, 032101 (2016).
- [51] Y. Baek, Y. Kafri, and V. Lecomte, Dynamical phase transitions in the current distribution of driven diffusive channels, *J. Phys. A: Math. Theor.* **51**, 105001 (2018).

# Supplementary Material: Hydrodynamics of a hard-core non-polar active lattice gas

Ritwik Mukherjee,<sup>1,\*</sup> Soumyabrata Saha,<sup>2,†</sup> Tridib Sadhu,<sup>2,‡</sup> Abhishek Dhar,<sup>1,§</sup> and Sanjib Sabhapandit<sup>3,¶</sup>

<sup>1</sup>*International Centre for Theoretical Sciences, Tata Institute of Fundamental Research, Bangalore 560089, India*

<sup>2</sup>*Department of Theoretical Physics, Tata Institute of Fundamental Research, Mumbai 400005, India*

<sup>3</sup>*Raman Research Institute, Bangalore 560080, India*

(Dated: May 31, 2024)

We present additional analytical and numerical details complementing the results presented in the main text of the *Letter*. These include a detailed derivation of the fluctuating hydrodynamics, the spinodal and binodal analysis, a derivation of the spatial correlations, and details about Monte Carlo and numerical iteration of the hydrodynamics.

## CONTENTS

S-1. Fluctuating hydrodynamics for the quasi-1D model: An Action formulation	S-1
A. The hydrodynamic limit	S-3
S-2. Generalisation to $d$ -dimensions	S-6
A. Case I: 2-species generalisation	S-6
B. Case II: $2d$ -species generalisation	S-7
S-3. The strictly-1D model with exchange dynamics	S-7
S-4. The spinodal analysis	S-8
S-5. The binodal analysis	S-9
A. First relation	S-10
B. Second relation	S-11
S-6. The two-point correlations in the stationary-state homogeneous phase	S-12
S-7. Details of the numerical simulations	S-16
References	S-16

## S-1. FLUCTUATING HYDRODYNAMICS FOR THE QUASI-1D MODEL: AN ACTION FORMULATION

Here, we present a derivation of the fluctuating hydrodynamic description for the quasi-1D model introduced in the *Letter*, following a similar route that was used earlier in [1] for the finite-line SSEP with slow boundaries. The dynamics of our model is defined in items (1-3) of the *Letter* and schematically shown in Fig. (1) of the *Letter*.

The configuration of the system at any time  $\tau$  is described by  $\mathbf{n}(\tau) \equiv \{n_{i,j}^+(\tau), n_{i,j}^-(\tau)\}$  where the occupation variables take the values

$$(n_{i,j}^+(\tau), n_{i,j}^-(\tau)) = \{(1, 0), (0, 1), (0, 0)\} \quad (\text{S-1})$$

depending on whether the  $i$ -th site of  $j$ -lane is occupied by a particle of species (+) or (−), or unoccupied respectively. This ensures that at any given time, no more than one particle of either species occupies a site. The stochastic evolution

\* ritwik.mukherjee@icts.res.in

† soumyabrata.saha@tifr.res.in

‡ tridib@theory.tifr.res.in

§ abhishek.dhar@icts.res.in

¶ sanjib@rri.res.in



$(\mathcal{B}_{i,1}^+, \mathcal{B}_{i,1}^-, \mathcal{B}_{i,2}^+, \mathcal{B}_{i,2}^-, \mathcal{T}_{i,1}, \mathcal{T}_{i,2}, \mathcal{L}_i^+, \mathcal{L}_i^-)$	Rate
$(1, 0, 0, 0, 0, 0, 0, 0)$	$\tau_p^{-1} (\ell_d^2 + \ell_p/2) n_{i,1}^+ (1 - n_{i+1,1}^+ - n_{i+1,1}^-)$
$(-1, 0, 0, 0, 0, 0, 0, 0)$	$\tau_p^{-1} (\ell_d^2 - \ell_p/2) n_{i+1,1}^+ (1 - n_{i,1}^+ - n_{i,1}^-)$
$(0, 1, 0, 0, 0, 0, 0, 0)$	$\tau_p^{-1} (\ell_d^2 - \ell_p/2) n_{i,1}^- (1 - n_{i+1,1}^+ - n_{i+1,1}^-)$
$(0, -1, 0, 0, 0, 0, 0, 0)$	$\tau_p^{-1} (\ell_d^2 + \ell_p/2) n_{i+1,1}^- (1 - n_{i,1}^+ - n_{i,1}^-)$
$(0, 0, 1, 0, 0, 0, 0, 0)$	$\tau_p^{-1} (\ell_d^2 + \ell_p/2) n_{i,2}^+ (1 - n_{i+1,2}^+ - n_{i+1,2}^-)$
$(0, 0, -1, 0, 0, 0, 0, 0)$	$\tau_p^{-1} (\ell_d^2 - \ell_p/2) n_{i+1,2}^+ (1 - n_{i,2}^+ - n_{i,2}^-)$
$(0, 0, 0, 1, 0, 0, 0, 0)$	$\tau_p^{-1} (\ell_d^2 - \ell_p/2) n_{i,2}^- (1 - n_{i+1,2}^+ - n_{i+1,2}^-)$
$(0, 0, 0, -1, 0, 0, 0, 0)$	$\tau_p^{-1} (\ell_d^2 + \ell_p/2) n_{i+1,2}^- (1 - n_{i,2}^+ - n_{i,2}^-)$
$(0, 0, 0, 0, \pm 1, 0, 0, 0)$	$\tau_p^{-1} n_{i,1}^\pm$
$(0, 0, 0, 0, 0, \pm 1, 0, 0)$	$\tau_p^{-1} n_{i,2}^\pm$
$(0, 0, 0, 0, 0, 0, 1, 0)$	$\tau_\times^{-1} n_{i,1}^+ (1 - n_{i,2}^+ - n_{i,2}^-)$
$(0, 0, 0, 0, 0, 0, -1, 0)$	$\tau_\times^{-1} n_{i,2}^+ (1 - n_{i,1}^+ - n_{i,1}^-)$
$(0, 0, 0, 0, 0, 0, 0, 1)$	$\tau_\times^{-1} n_{i,1}^- (1 - n_{i,2}^+ - n_{i,2}^-)$
$(0, 0, 0, 0, 0, 0, 0, -1)$	$\tau_\times^{-1} n_{i,2}^- (1 - n_{i,1}^+ - n_{i,1}^-)$

TABLE S-1. Possible values of the various dynamical events for the quantities in (S-2) and corresponding rates.

of the system configuration relates to biased hops, tumblings and lane-crossings as

$$n_{i,1}^\pm(\tau + d\tau) - n_{i,1}^\pm(\tau) = \mathcal{B}_{i-1,1}^\pm(\tau) - \mathcal{B}_{i,1}^\pm(\tau) \mp \mathcal{T}_{i,1}(\tau) - \mathcal{L}_i^\pm(\tau) \quad (\text{S-2a})$$

$$n_{i,2}^\pm(\tau + d\tau) - n_{i,2}^\pm(\tau) = \mathcal{B}_{i-1,2}^\pm(\tau) - \mathcal{B}_{i,2}^\pm(\tau) \mp \mathcal{T}_{i,2}(\tau) + \mathcal{L}_i^\pm(\tau) \quad (\text{S-2b})$$

where,  $\mathcal{B}_{i,j}^\sigma$  corresponds to the **biased-hopping** event of a  $\sigma$ -species particle between the  $i^{\text{th}}$  and  $i+1^{\text{th}}$  sites of  $j$ -lane,  $\mathcal{T}_{i,j}$  corresponds to the **tumbling** event of a particle at the  $i^{\text{th}}$  site of  $j$ -lane and  $\mathcal{L}_i^\sigma$  corresponds to the **lane-crossing** event of a  $\sigma$ -species particle between the  $i^{\text{th}}$  sites of the two lanes. For an infinitesimal  $d\tau$ , the various possible values that these variables can take are listed in Table S-1.

Our interest lies in determining the probability that the system starting from an initial configuration  $\mathbf{n}(0)$  evolves into a final configuration  $\mathbf{n}(T)$ . This transition probability can be written as a path integral over all possible evolution trajectories  $\{\mathbf{n}(\tau), \mathcal{B}(\tau), \mathcal{T}(\tau), \mathcal{L}(\tau)\}$  as

$$\begin{aligned} \Pr[\mathbf{n}(T) | \mathbf{n}(0)] = \int_{\mathbf{n}(0)}^{\mathbf{n}(T)} [\mathcal{D}\mathbf{n}] & \left\langle \prod_{\tau=0}^{T-d\tau} \prod_{i=1}^L \left( \delta_{n_{i,1}^+(\tau+d\tau)-n_{i,1}^+(\tau), \mathcal{B}_{i-1,1}^+(\tau)-\mathcal{B}_{i,1}^+(\tau)-\mathcal{T}_{i,1}(\tau)-\mathcal{L}_i^+(\tau)} \right. \right. \\ & \times \delta_{n_{i,1}^-(\tau+d\tau)-n_{i,1}^-(\tau), \mathcal{B}_{i-1,1}^-(\tau)-\mathcal{B}_{i,1}^-(\tau)+\mathcal{T}_{i,1}(\tau)-\mathcal{L}_i^-(\tau)} \\ & \times \delta_{n_{i,2}^+(\tau+d\tau)-n_{i,2}^+(\tau), \mathcal{B}_{i-1,2}^+(\tau)-\mathcal{B}_{i,2}^+(\tau)-\mathcal{T}_{i,2}(\tau)+\mathcal{L}_i^+(\tau)} \\ & \left. \left. \times \delta_{n_{i,2}^-(\tau+d\tau)-n_{i,2}^-(\tau), \mathcal{B}_{i-1,2}^-(\tau)-\mathcal{B}_{i,2}^-(\tau)+\mathcal{T}_{i,2}(\tau)+\mathcal{L}_i^-(\tau)} \right) \right\rangle_{\{\mathcal{B}(\tau), \mathcal{T}(\tau), \mathcal{L}(\tau)\}} \quad (\text{S-3}) \end{aligned}$$



where the path integral measure on the occupation variables is defined as

$$\int [\mathcal{D}\mathbf{n}] := \prod_{\tau=0}^T \prod_{i=1}^L \prod_{j=1}^2 \prod_{\sigma=(\pm)} \sum_{n_{i,j}^{\sigma}(\tau)=0}^1 \quad (\text{S-4})$$

Using an integral representation of the Kronecker-delta function  $\delta_{a,b} = (2\pi i)^{-1} \int_{-\pi}^{i\pi} dz e^{-z(a-b)}$  and then, performing the averages over the variables  $\mathcal{B}_{i,j}^{\sigma}$ ,  $\mathcal{T}_{i,j}$  and  $\mathcal{L}^{\sigma}$  using Table S-1, we can write the exact path integral description of the configuration's transition probability in terms of an exact microscopic Action

$$\Pr[\mathbf{n}(T) | \mathbf{n}(0)] = \int_{\mathbf{n}(0)}^{\mathbf{n}(T)} [\mathcal{D}\mathbf{n}] [\mathcal{D}\hat{\mathbf{n}}] e^{\mathcal{K}[\mathbf{n}, \hat{\mathbf{n}}] + \mathcal{H}[\mathbf{n}, \hat{\mathbf{n}}]} \quad (\text{S-5a})$$

with the ‘‘kinetic’’ term

$$\mathcal{K} = \sum_{i=1}^L \sum_{j=1}^2 \sum_{\sigma=(\pm)} \left[ n_{i,j}^{\sigma}(0) \hat{n}_{i,j}^{\sigma}(0) - n_{i,j}^{\sigma}(T) \hat{n}_{i,j}^{\sigma}(T) + \int_0^T d\tau \left( n_{i,j}^{\sigma}(\tau) \frac{d\hat{n}_{i,j}^{\sigma}(\tau)}{d\tau} \right) \right] \quad (\text{S-5b})$$

and the ‘‘Hamiltonian’’ term

$$\begin{aligned} \mathcal{H} = & \frac{\ell_d^2}{\tau_p} \sum_{i=1}^L \sum_{j=1}^2 \sum_{\sigma=(\pm)} \int_0^T d\tau \left[ (e^{\hat{n}_{i+1,j}^{\sigma} - \hat{n}_{i,j}^{\sigma}} - 1) n_{i,j}^{\sigma} (1 - n_{i+1,j}) + (e^{\hat{n}_{i,j}^{\sigma} - \hat{n}_{i+1,j}^{\sigma}} - 1) n_{i+1,j}^{\sigma} (1 - n_{i,j}) \right] \\ & + \frac{\ell_p}{2\tau_p} \sum_{i=1}^L \sum_{j=1}^2 \int_0^T d\tau \left[ (e^{\hat{n}_{i+1,j}^+ - \hat{n}_{i,j}^+} - 1) n_{i,j}^+ (1 - n_{i+1,j}) - (e^{\hat{n}_{i,j}^+ - \hat{n}_{i+1,j}^+} - 1) n_{i+1,j}^+ (1 - n_{i,j}) \right. \\ & \quad \left. - (e^{\hat{n}_{i+1,j}^- - \hat{n}_{i,j}^-} - 1) n_{i,j}^- (1 - n_{i+1,j}) + (e^{\hat{n}_{i,j}^- - \hat{n}_{i+1,j}^-} - 1) n_{i+1,j}^- (1 - n_{i,j}) \right] \\ & + \frac{1}{\tau_p} \sum_{i=1}^L \sum_{j=1}^2 \int_0^T d\tau \left[ (e^{\hat{n}_{i,j}^- - \hat{n}_{i,j}^+} - 1) n_{i,j}^+ + (e^{\hat{n}_{i,j}^+ - \hat{n}_{i,j}^-} - 1) n_{i,j}^- \right] \\ & + \frac{1}{\tau_{\times}} \sum_{i=1}^L \sum_{\sigma=(\pm)} \int_0^T d\tau \left[ (e^{\hat{n}_{i,2}^{\sigma} - \hat{n}_{i,1}^{\sigma}} - 1) n_{i,1}^{\sigma} (1 - n_{i,2}) + (e^{\hat{n}_{i,1}^{\sigma} - \hat{n}_{i,2}^{\sigma}} - 1) n_{i,2}^{\sigma} (1 - n_{i,1}) \right] \end{aligned} \quad (\text{S-5c})$$

where we have denoted  $n_{i,j}(\tau) = \sum_{\sigma} n_{i,j}^{\sigma}(\tau)$  as the total occupation number of the  $i^{\text{th}}$  site of  $j$ -lane at time  $\tau$  and the path integral measure on the conjugate response variable is defined as

$$\int [\mathcal{D}\hat{\mathbf{n}}] := \prod_{\tau=0}^T \prod_{i=1}^L \prod_{j=1}^2 \prod_{\sigma=(\pm)} \frac{1}{2\pi i} \int_{-\pi}^{i\pi} d\hat{n}_{i,j}^{\sigma}(\tau) \quad (\text{S-6})$$

### A. The hydrodynamic limit

Given the diffusive nature of the dynamics for our quasi-1D model, the occupation variables in a region of length-scale  $\sim \ell_d$  reach a local equilibrium over a period of time-scale  $\sim \tau_p$  with respect to a slowly varying density profile. In this scale, this local equilibrium measure that governs the distribution of occupation variables is given by

$$(n_{i,j}^+(\tau), n_{i,j}^-(\tau)) = \begin{cases} (1, 0) & \text{with prob. } \rho_i^+(\tau) \equiv \rho_+ \left( \frac{i}{\ell_d}, \frac{\tau}{\tau_p} \right) & (\text{S-7a}) \\ (0, 1) & \text{with prob. } \rho_i^-(\tau) \equiv \rho_- \left( \frac{i}{\ell_d}, \frac{\tau}{\tau_p} \right) & (\text{S-7b}) \\ (0, 0) & \text{with prob. } 1 - \rho_i(\tau) \equiv 1 - \rho \left( \frac{i}{\ell_d}, \frac{\tau}{\tau_p} \right) & (\text{S-7c}) \end{cases}$$

It is important to note here that the local equilibrium measure followed by the occupation variables in the two lanes is identical. This is because the particles cross between lanes more frequently than either making biased-hops or tumbling in one lane, thereby leading to a fast equilibration between the two lanes. Consequently, we also consider

the response variables to be approximated by slowly varying response fields which are identical for the two lanes in the hydrodynamic length ( $\sim \ell_d$ ) and time ( $\sim \tau_p$ ) scales

$$\hat{n}_{i,j}^{\pm}(\tau) \simeq \hat{\rho}_i^{\pm}(\tau) \equiv \hat{\rho}_{\pm}\left(\frac{i}{\ell_d}, \frac{\tau}{\tau_p}\right) \quad (\text{S-8})$$

In the hydrodynamic scale, the initial and final configurations typically follow the slowly varying density profiles  $\rho(i/\ell_d, 0)$  and  $\rho(i/\ell_d, T/\tau_p)$  respectively, such that for large  $\ell_d$  and  $\tau_p$ , we can write

$$\sum_{i=1}^L n_{i,j}^{\sigma}(0) \hat{n}_{i,j}^{\sigma}(0) \simeq \sum_{i=1}^L \rho_i^{\sigma}(0) \hat{\rho}_i^{\sigma}(0) \quad \text{and} \quad \sum_{i=1}^L n_{i,j}^{\pm}(T) \hat{n}_{i,j}^{\sigma}(T) \simeq \sum_{i=1}^L \rho_i^{\sigma}(T) \hat{\rho}_i^{\sigma}(T) \quad (\text{S-9})$$

where we have used the fact that the response variables for the two lanes follow the same slowly varying response field.

In the leading order for large  $\ell_d$  and  $\tau_p$ , the transition probability in the system configuration is given by the exact microscopic expression in (S-5a) averaged over the occupation variables using the local equilibrium measure (S-7) as

$$\Pr[\boldsymbol{\rho}(T) | \boldsymbol{\rho}(0)] = \int_{\boldsymbol{\rho}(0)}^{\boldsymbol{\rho}(T)} [\mathcal{D}\boldsymbol{\rho}] [\mathcal{D}\hat{\boldsymbol{\rho}}] \left\langle e^{\mathcal{K}[\mathbf{n}, \hat{\boldsymbol{\rho}}] + \mathcal{H}[\mathbf{n}, \hat{\boldsymbol{\rho}}]} \right\rangle_{\{\mathbf{n}(\tau)\}} \quad (\text{S-10})$$

with  $\mathcal{K}$  and  $\mathcal{H}$  as given in (S-5b) and (S-5c) respectively, but with  $\hat{n}_{i,j}^{\sigma}(\tau)$  replaced by  $\hat{\rho}_i^{\sigma}(\tau)$  due to (S-8).

In order to perform the averaging, we assume that for large  $\ell_d$  and  $\tau_p$ , the probability measure at different times are independent of one another such that the leading order behaviour of the transition probability can be written as

$$\Pr[\boldsymbol{\rho}(T) | \boldsymbol{\rho}(0)] = \int_{\boldsymbol{\rho}(0)}^{\boldsymbol{\rho}(T)} [\mathcal{D}\boldsymbol{\rho}] [\mathcal{D}\hat{\boldsymbol{\rho}}] \exp \left[ 2 \sum_{i=1}^L \sum_{\sigma=(\pm)} \left( \rho_i^{\sigma}(0) \hat{\rho}_i^{\sigma}(0) - \rho_i^{\sigma}(T) \hat{\rho}_i^{\sigma}(T) \right) \right] \prod_{\tau=0}^{T-d\tau} \left\langle e^{d\tau \mathcal{S}(\tau)} \right\rangle_{\mathbf{n}(\tau)} \quad (\text{S-11a})$$

with the Action

$$\begin{aligned} \mathcal{S} = & \sum_{i=1}^L \sum_{j=1}^2 \sum_{\sigma=(\pm)} \left( n_{i,j}^{\sigma}(\tau) \frac{d\hat{\rho}_i^{\sigma}(\tau)}{d\tau} \right) \\ & + \frac{\ell_d^2}{\tau_p} \sum_{i=1}^L \sum_{j=1}^2 \sum_{\sigma=(\pm)} \left[ \left( e^{\hat{\rho}_{i+1}^{\sigma} - \hat{\rho}_i^{\sigma}} - 1 \right) n_{i,j}^{\sigma} (1 - n_{i+1,j}) + \left( e^{\hat{\rho}_i^{\sigma} - \hat{\rho}_{i+1}^{\sigma}} - 1 \right) n_{i+1,j}^{\sigma} (1 - n_{i,j}) \right] \\ & + \frac{\ell_p}{2\tau_p} \sum_{i=1}^L \sum_{j=1}^2 \left[ \left( e^{\hat{\rho}_{i+1}^+ - \hat{\rho}_i^+} - 1 \right) n_{i,j}^+ (1 - n_{i+1,j}) - \left( e^{\hat{\rho}_i^+ - \hat{\rho}_{i+1}^+} - 1 \right) n_{i+1,j}^+ (1 - n_{i,j}) \right. \\ & \quad \left. - \left( e^{\hat{\rho}_{i+1}^- - \hat{\rho}_i^-} - 1 \right) n_{i,j}^- (1 - n_{i+1,j}) + \left( e^{\hat{\rho}_i^- - \hat{\rho}_{i+1}^-} - 1 \right) n_{i+1,j}^- (1 - n_{i,j}) \right] \\ & + \frac{1}{\tau_p} \sum_{i=1}^L \sum_{j=1}^2 \left[ \left( e^{\hat{\rho}_i^- - \hat{\rho}_i^+} - 1 \right) n_{i,j}^+ + \left( e^{\hat{\rho}_i^+ - \hat{\rho}_i^-} - 1 \right) n_{i,j}^- \right] \end{aligned} \quad (\text{S-11b})$$

where we have made use of (S-9). It must be noted here that due to the fast equilibration between the two lanes as in (S-8), the lane-crossing ( $\tau_{\times}$ ) term in the Hamiltonian vanishes.

We can further simplify the averaging in (S-11a) by noting that in the limit  $d\tau \rightarrow 0$  limit, we have

$$\prod_{\tau} \left\langle e^{d\tau \mathcal{S}(\tau)} \right\rangle_{\mathbf{n}(\tau)} \simeq \prod_{\tau} e^{d\tau \mathcal{S}(\tau)_{\mathbf{n}(\tau)}} \quad (\text{S-12})$$

With this, the task of averaging over the occupation variables boils down to  $n_{i,1}^{\pm}(\tau)$  and  $n_{i,2}^{\pm}(\tau)$  being replaced by  $\rho_i^{\pm}(\tau)$  in (S-11b), which gives

$$\Pr[\boldsymbol{\rho}(T) | \boldsymbol{\rho}(0)] = \int_{\boldsymbol{\rho}(0)}^{\boldsymbol{\rho}(T)} [\mathcal{D}\boldsymbol{\rho}] [\mathcal{D}\hat{\boldsymbol{\rho}}] e^{2 \int_0^T d\tau \sum_{i=1}^L \mathcal{S}(\rho_i^{\pm}(\tau), \hat{\rho}_i^{\pm}(\tau))} \quad (\text{S-13a})$$

where the Action is

$$\begin{aligned}
\mathcal{S}(\rho_i^\pm(\tau), \hat{\rho}_i^\pm(\tau)) = & -\hat{\rho}_i^+ \frac{d\rho_i^+}{d\tau} - \hat{\rho}_i^- \frac{d\rho_i^-}{d\tau} \\
& + \frac{\ell_d^2}{\tau_p} \left[ (e^{\hat{n}_{i+1}^- - \hat{n}_i^-} - 1) n_i^- (1 - n_{i+1}) + (e^{\hat{n}_i^- - \hat{n}_{i+1}^-} - 1) n_{i+1}^- (1 - n_i) \right. \\
& \quad \left. + (e^{\hat{n}_{i+1}^- - \hat{n}_i^-} - 1) n_i^- (1 - n_{i+1}) + (e^{\hat{n}_i^- - \hat{n}_{i+1}^-} - 1) n_{i+1}^- (1 - n_i) \right] \\
& + \frac{\ell_p}{2\tau_p} \left[ (e^{\hat{n}_{i+1}^+ - \hat{n}_i^+} - 1) n_i^+ (1 - n_{i+1}) - (e^{\hat{n}_i^+ - \hat{n}_{i+1}^+} - 1) n_{i+1}^+ (1 - n_i) \right. \\
& \quad \left. - (e^{\hat{n}_{i+1}^- - \hat{n}_i^-} - 1) n_i^- (1 - n_{i+1}) + (e^{\hat{n}_i^- - \hat{n}_{i+1}^-} - 1) n_{i+1}^- (1 - n_i) \right] \\
& + \frac{1}{\tau_p} \left[ (e^{\hat{n}_{i,j}^- - \hat{n}_{i,j}^+} - 1) n_{i,j}^+ + (e^{\hat{n}_{i,j}^+ - \hat{n}_{i,j}^-} - 1) n_{i,j}^- \right] \tag{S-13b}
\end{aligned}$$

where we used an integration by parts in the  $\tau$ -variable to cancel out the exponential term outside the averaging in (S-11a).

The path integral description for the transition probability of the hydrodynamic density profiles is then obtained by performing a gradient expansion for large  $\ell_d$  and  $\tau_p$

$$\Pr[\rho_\pm(x, \mathbb{T}) | \rho_\pm(x, 0)] = \int_{\rho_\pm(x, 0)}^{\rho_\pm(x, \mathbb{T})} [\mathcal{D}\rho_\pm] [\mathcal{D}\hat{\rho}_\pm] e^{-2\ell_d \int_0^\mathbb{T} dt \left[ \int_0^L dx (\hat{\rho}_+ \partial_t \rho_+ + \hat{\rho}_- \partial_t \rho_-) - H[\hat{\rho}_\pm, \rho_\pm] \right]} \tag{S-14a}$$

with the Hamiltonian given by

$$\begin{aligned}
H = \int_0^L dx \left\{ \rho_+ (1 - \rho) (\partial_x \hat{\rho}_+)^2 + \rho_- (1 - \rho) (\partial_x \hat{\rho}_-)^2 - [(1 - \rho_-) \partial_x \rho_+ + \rho_+ \partial_x \rho_- - \text{Pe} \rho_+ (1 - \rho)] \partial_x \hat{\rho}_+ \right. \\
\left. - [(1 - \rho_+) \partial_x \rho_- + \rho_- \partial_x \rho_+ + \text{Pe} \rho_- (1 - \rho)] \partial_x \hat{\rho}_- + (e^{-\hat{\rho}_+ + \hat{\rho}_-} - 1) \rho_+ + (e^{\hat{\rho}_+ - \hat{\rho}_-} - 1) \rho_- \right\} \tag{S-14b}
\end{aligned}$$

where we have denoted  $T\tau_p^{-1} = \mathbb{T}$  and  $L\ell_d^{-1} = \mathbb{L}$ .

In order to write the hydrodynamic transition probability in terms of the total density ( $\rho = \rho_+ + \rho_-$ ) and polarisation ( $m = \rho_+ - \rho_-$ ) fields, we define the corresponding response fields as  $\hat{\rho} = (\hat{\rho}_+ + \hat{\rho}_-)/2$  and  $\hat{m} = (\hat{\rho}_+ - \hat{\rho}_-)/2$  respectively. This gives us

$$\Pr[\rho(x, \mathbb{T}), m(x, \mathbb{T}) | \rho(x, 0), m(x, 0)] \simeq \int_{\rho(x, 0), m(x, 0)}^{\rho(x, \mathbb{T}), m(x, \mathbb{T})} [\mathcal{D}\rho] [\mathcal{D}m] [\mathcal{D}\hat{\rho}] [\mathcal{D}\hat{m}] e^{-2\ell_d \int_0^\mathbb{T} dt \left[ \int_0^L dx (\hat{\rho} \partial_t \rho + \hat{m} \partial_t m) - H[\hat{\rho}, \hat{m}, \rho, m] \right]} \tag{S-15a}$$

with the Hamiltonian

$$\begin{aligned}
H = \int_0^L dx \left\{ \rho(1 - \rho) (\partial_x \hat{\rho})^2 + \rho(1 - \rho) (\partial_x \hat{m})^2 + 2m(1 - \rho) \partial_x \hat{\rho} \partial_x \hat{m} - [\partial_x \rho - \text{Pe} m (1 - \rho)] \partial_x \hat{\rho} \right. \\
\left. - [(1 - \rho) \partial_x m + m \partial_x \rho - \text{Pe} \rho (1 - \rho)] \partial_x \hat{m} + 2\rho \sinh^2 \hat{m} - m \sinh 2\hat{m} \right\} \tag{S-15b}
\end{aligned}$$

In order to characterise fluctuations which are up to Gaussian order only, we make the quadratic approximation by keeping terms which are at most quadratic in the response fields such that the Hamiltonian reduces to

$$H[\hat{\rho}, \hat{m}, \rho, m] = \int_0^{L/\ell_d} dx \left[ \frac{S_{\rho, \rho}}{2} (\partial_x \hat{\rho})^2 + \frac{S_{m, m}}{2} (\partial_x \hat{m})^2 + S_{\rho, m} \partial_x \hat{\rho} \partial_x \hat{m} + 2S_{f, f} \hat{m}^2 + \bar{J}_\rho \partial_x \hat{\rho} + \bar{J}_m \partial_x \hat{m} - 2\bar{J}_f \hat{m} \right] \tag{S-16a}$$

with

$$S_{\rho, \rho} = S_{m, m} = 2\rho(1 - \rho) \tag{S-16b}$$

$$S_{\rho, m} = 2m(1 - \rho) \tag{S-16c}$$

$$S_{f, f} = \rho \tag{S-16d}$$

$$\bar{J}_\rho = -\partial_x \rho + \text{Pe} m (1 - \rho) \tag{S-16e}$$

$$\bar{J}_m = -(1 - \rho) \partial_x m - m \partial_x \rho + \text{Pe} \rho (1 - \rho) \tag{S-16f}$$

$$\bar{J}_f = m \tag{S-16g}$$

We can now write the corresponding fluctuating hydrodynamics for our quasi-1D model by inverting the MSRJD-Action in (S-15a) with the Hamiltonian in (S-16). This is given as

$$\partial_t \rho = -\partial_x \left( \bar{J}_\rho - \frac{1}{\sqrt{\ell_d}} \eta_\rho \right) \quad (\text{S-17a})$$

$$\partial_t m = -\partial_x \left( \bar{J}_m - \frac{1}{\sqrt{\ell_d}} \eta_m \right) - 2 \left( \bar{J}_f - \frac{1}{\sqrt{\ell_d}} \eta_f \right) \quad (\text{S-17b})$$

where the noise vector  $\boldsymbol{\eta} \equiv (\eta_\rho \ \eta_m \ \eta_f)^\text{T}$  is a multivariate Gaussian noise-vector whose probability distribution is

$$\text{Pr}(\boldsymbol{\eta}) \sim \exp \left\{ -\frac{1}{2} \int dt dt' dx dx' [(\boldsymbol{\eta}(x, t) - \boldsymbol{\mu})^\text{T} \boldsymbol{\Sigma}^{-1} (\boldsymbol{\eta}(x', t') - \boldsymbol{\mu})] \right\} \quad (\text{S-18})$$

with the mean-vector and the covariance-matrix respectively

$$\boldsymbol{\mu} = \begin{pmatrix} 0 \\ 0 \\ 0 \end{pmatrix} \quad \text{and} \quad \boldsymbol{\Sigma} = \delta(x - x') \delta(t - t') \begin{pmatrix} S_{\rho, \rho} & S_{\rho, m} & 0 \\ S_{\rho, m} & S_{m, m} & 0 \\ 0 & 0 & S_{f, f} \end{pmatrix} \quad (\text{S-19})$$

## S-2. GENERALISATION TO $d$ -DIMENSIONS

Here, we generalise the Action formalism and thus, the fluctuating hydrodynamic description for our model on a  $d$ -dimensional hyper-cubic lattice with  $L^d$  sites with periodic boundaries. The lattice sites are indexed as  $(i_1, i_2, \dots, i_d)$  with  $i_k = \{1, 2, \dots, L\}$  for  $k = 1, 2, \dots, d$ . We discuss two possible generalisations as mentioned in the *Letter*.

### A. Case I: 2-species generalisation

This case corresponds to the case where the system is composed of particles of 2-species (denoted as  $(\pm)$ ) similar to the quasi-1D model. The  $(\pm)$  particles move persistently in the  $\pm \hat{x}_1$  direction (which we refer to as *active* direction) with the motion being symmetric along all other directions  $\{\pm \hat{x}_2, \dots, \pm \hat{x}_d\}$  (which we refer to as *passive* directions). The microscopic dynamics is defined as

- *Biased-Hopping*: A  $(+)$  particle at site  $(i_1, i_2, \dots, i_d)$  hops to the site  $(i_1 \pm 1, i_2, \dots, i_d)$  at rate  $(\ell_d^2 \pm \ell_p/2)/\tau_p$  and to the sites  $(i_1, i_2 \pm 1, \dots, i_d), \dots, (i_1, i_2, \dots, i_d \pm 1)$  at rate  $\ell_d^2/\tau_p$ , while a  $(-)$  particle at site  $(i_1, i_2, \dots, i_d)$  hops to the site  $(i_1 \pm 1, i_2, \dots, i_d)$  at rate  $(\ell_d^2 \mp \ell_p/2)/\tau_p$  and to the sites  $(i_1, i_2 \pm 1, \dots, i_d), \dots, (i_1, i_2, \dots, i_d \pm 1)$  at rate  $\ell_d^2/\tau_p$ , provided that the target site is unoccupied
- *Tumbling*: A  $(+)$  particle converts to a  $(-)$  particle at rate  $1/\tau_p$  and vice-versa

Starting from an initial configuration  $\rho_\pm(x, t_{\text{ini}})$ , the probability that the system eventually reaches a final configuration  $\rho_\pm(x, t_{\text{fin}})$  has a hydrodynamic path integral description

$$\text{Pr} [\rho_\pm(\vec{x}, t_{\text{fin}}) | \rho_\pm(\vec{x}, t_{\text{ini}})] = \int [\mathcal{D}\rho_\pm] [\mathcal{D}\hat{\rho}_\pm] e^{-\ell_d^d \int dt \int d\vec{x} (\hat{\rho}_+ \partial_t \rho_+ + \hat{\rho}_- \partial_t \rho_-) - H[\hat{\rho}_\pm, \rho_\pm]} \quad (\text{S-20a})$$

with the Hamiltonian given by

$$H = \int d\vec{x} \left\{ \rho_+ (1 - \rho) |\vec{\nabla} \hat{\rho}_+|^2 + \rho_- (1 - \rho) |\vec{\nabla} \hat{\rho}_-|^2 - [(1 - \rho_-) \vec{\nabla} \rho_+ + \rho_+ \vec{\nabla} \rho_- - \text{Pe} \rho_+ (1 - \rho) \hat{x}_1] \cdot \vec{\nabla} \hat{\rho}_+ \right. \\ \left. - [(1 - \rho_+) \vec{\nabla} \rho_- + \rho_- \vec{\nabla} \rho_+ + \text{Pe} \rho_- (1 - \rho) \hat{x}_1] \cdot \vec{\nabla} \hat{\rho}_- + (e^{-\hat{\rho}_+ + \hat{\rho}_-} - 1) \rho_+ + (e^{\hat{\rho}_+ - \hat{\rho}_-} - 1) \rho_- \right\} \quad (\text{S-20b})$$

and where we have denoted  $\rho = \rho_+ + \rho_-$ .

The fluctuating hydrodynamic equations corresponding to this Action formalism is then given by

$$\partial_t \rho_\pm = (1 - \rho) \nabla^2 \rho_\pm + \rho_\pm \nabla^2 \rho \mp \text{Pe} \partial_{x_1} [\rho_\pm (1 - \rho)] \mp (\rho_+ - \rho_-) + \frac{1}{\ell_d^{d/2}} (\vec{\nabla} \cdot \vec{\eta}_\pm \pm \eta_f) \quad (\text{S-21})$$

with the Gaussian noises having zero means and covariances

$$\left\langle (\vec{\eta}_\pm(\vec{x}, t) \cdot \hat{x}_k) (\vec{\eta}_\pm(\vec{x}', t') \cdot \hat{x}_{k'}) \right\rangle = 2 \rho_\pm (1 - \rho) \delta_{k, k'} \delta(\vec{x} - \vec{x}') \delta(t - t') \\ \left\langle \eta_f(\vec{x}, t) \eta_f(\vec{x}', t') \right\rangle = \rho \delta(\vec{x} - \vec{x}') \delta(t - t') \quad (\text{S-22})$$



## B. Case II: 2d-species generalisation

In this generalisation, the system is composed of particles belonging to  $2d$  number of species (denoted as  $\sigma = \{(\pm)_k\}$  with  $k = 1, 2, \dots, d$ ), corresponding to the possible internal orientations in the spatial directions  $\hat{r}_k = \{\pm \hat{x}_k\}$  with  $k = 1, 2, \dots, d$ . This corresponds to the isotropic generalisation of our quasi-1D model in higher dimensions. The microscopic dynamics is defined as

- *Biased-Hopping*: A particle of  $(+)_k$  species at site  $(i_1, i_2, \dots, i_d)$  hops to the site  $(i_1, i_2, \dots, i_k + 1, \dots, i_d)$  at rate  $(\ell_d^2 + \ell_p/2)/\tau_p$  and to the other adjacent sites at rate  $(\ell_d^2 - \ell_p/2)/\tau_p$ , while a particle of  $(-)_k$  species at site  $(i_1, i_2, \dots, i_d)$  hops to the site  $(i_1, i_2, \dots, i_k - 1, \dots, i_d)$  at rate  $(\ell_d^2 + \ell_p/2)/\tau_p$  and to the other adjacent sites at rate  $(\ell_d^2 - \ell_p/2)/\tau_p$ , provided that the target site is unoccupied
- *Tumbling*: A particle of  $\sigma$  species converts to any other species at rate  $1/\tau_p$

Starting from an initial configuration  $\rho_\sigma(x, t_{\text{ini}})$ , the probability that the system eventually reaches a final configuration  $\rho_\sigma(x, t_{\text{fin}})$  has a hydrodynamic path integral description

$$\Pr [\rho_\sigma(\vec{x}, t_{\text{fin}}) | \rho_\sigma(\vec{x}, t_{\text{ini}})] \simeq \int [\mathcal{D}\rho] [\mathcal{D}\hat{\rho}] e^{-\ell_d^d \int dt [\int d\vec{x} \sum_\sigma (\hat{\rho}_\sigma \partial_t \rho_\sigma) - H[\rho_\sigma, \hat{\rho}_\sigma]}] \quad (\text{S-23a})$$

where the Hamiltonian is given by

$$H = \int d\vec{x} \sum_\sigma \left\{ \rho_\sigma (1 - \rho) |\vec{\nabla} \hat{\rho}_\sigma|^2 - [(1 - \rho) \vec{\nabla} \rho_\sigma + \rho_\sigma \vec{\nabla} \rho - \text{Pe} \rho_\sigma (1 - \rho) \hat{r}_\sigma] \cdot \vec{\nabla} \hat{\rho}_\sigma + \sum_{\sigma' \neq \sigma} \rho_\sigma (e^{\hat{\rho}_{\sigma'} - \hat{\rho}_\sigma} - 1) \right\} \quad (\text{S-23b})$$

and we have used  $\rho = \sum_\sigma \rho_\sigma$ .

Corresponding to this Action formalism, the fluctuating hydrodynamics for the  $\sigma$ -species particle is then given by

$$\partial_t \rho_\sigma = (1 - \rho) \nabla^2 \rho_\sigma + \rho_\sigma \nabla^2 \rho - \text{Pe} \vec{\nabla} [\rho_\sigma (1 - \rho)] \cdot \hat{r}_\sigma - \sum_{\sigma' \neq \sigma} (\rho_\sigma - \rho_{\sigma'}) + \frac{1}{\ell_d^{d/2}} \left( \vec{\nabla} \cdot \vec{\eta}_\sigma + \sum_{\sigma' \neq \sigma} \eta_{\sigma \rightarrow \sigma'} \right) \quad (\text{S-24})$$

with the Gaussian noises having zero means and covariances

$$\begin{aligned} \langle (\vec{\eta}_\sigma(\vec{x}, t) \cdot \hat{x}_k) (\vec{\eta}_{\sigma'}(\vec{x}', t') \cdot \hat{x}_{k'}) \rangle &= 2 \rho_\sigma (1 - \rho) \delta_{\sigma, \sigma'} \delta_{k, k'} \delta(\vec{x} - \vec{x}') \delta(t - t') \\ \langle \eta_{\sigma \rightarrow \sigma'}(\vec{x}, t) \eta_{\psi \rightarrow \psi'}(\vec{x}', t') \rangle &= (\rho_\sigma + \rho_{\sigma'}) \delta_{\sigma, \psi} \delta_{\sigma', \psi'} \delta(\vec{x} - \vec{x}') \delta(t - t') \end{aligned} \quad (\text{S-25})$$

### S-3. THE STRICTLY-1D MODEL WITH EXCHANGE DYNAMICS

Until now, we have imposed a constraint on the motion of the active particles in that two particles in adjacent sites are strictly forbidden from exchanging their positions. This ensures that the hard-core repulsion between the particles is respected. However, if one is interested in studying the dynamics of active particles through a channel whose width is a few orders more than the diameter of the particles. Motivated by this scenario, we present the Action-formalism and subsequently, the fluctuating hydrodynamic description for a case where two adjacent particles are allowed to exchange their positions at a constant rate in addition to the usual biased-hopping and tumbling dynamics. For our derivation, we consider the model on a one-dimensional lattice with the trivial generalization to higher dimensions being similar to the one discussed in the previous Section. Explicitly, the microscopic dynamics is now given as

- *Biased-Hopping*: A  $(+)$  particle at site  $i$  hops to site  $i \pm 1$  at rate  $(\ell_d^2 \pm \ell_p/2)/\tau_p$  while a  $(-)$  particle at site  $i$  hops to site  $i \pm 1$  at rate  $(\ell_d^2 \mp \ell_p/2)/\tau_p$ , provided that the target site is unoccupied
- *Tumbling*: A particle changes its internal orientation (i.e.  $(+)$  to  $(-)$  and vice-versa) at rate  $1/\tau_p$
- *Particle-Position-Exchanging*: A pair of  $(\pm)$  particles at sites  $i, i + 1$  exchanges their positions at rate  $\ell_e^2/\tau_p$

Following the same procedure outlined in Section S-1, we can now write the transition probability of the system starting from an initial configuration  $\rho_\pm(x, t_{\text{ini}})$  and reaching a final configuration  $\rho_\pm(x, t_{\text{fin}})$  in terms of a path integral

$$\Pr [\rho_\pm(x, t_{\text{fin}}) | \rho_\pm(x, t_{\text{ini}})] = \int [\mathcal{D}\rho_\pm] [\mathcal{D}\hat{\rho}_\pm] e^{-\ell_d^d \int dt [\int dx (\hat{\rho}_+ \partial_t \rho_+ + \hat{\rho}_- \partial_t \rho_-) - H[\hat{\rho}_\pm, \rho_\pm]}] \quad (\text{S-26a})$$

where the Hamiltonian is given by

$$\begin{aligned}
H = \int dx & [\rho_+ (1 - \rho) + \mathcal{E} \rho_+ \rho_-] (\partial_x \hat{\rho}_+)^2 + [\rho_- (1 - \rho) + \mathcal{E} \rho_+ \rho_-] (\partial_x \hat{\rho}_-)^2 - 2 \mathcal{E} \rho_+ \rho_- \partial_x \hat{\rho}_+ \partial_x \hat{\rho}_- \\
& - \left\{ [1 - \rho_- + \mathcal{E} \rho_-] \partial_x \rho_+ + (1 - \mathcal{E}) \rho_+ \partial_x \rho_- - \text{Pe} \rho_+ (1 - \rho) \right\} \partial_x \hat{\rho}_+ \\
& - \left\{ [1 - \rho_+ + \mathcal{E} \rho_+] \partial_x \rho_- + (1 - \mathcal{E}) \rho_- \partial_x \rho_+ + \text{Pe} \rho_- (1 - \rho) \right\} \partial_x \hat{\rho}_- \\
& + \rho_- (e^{\hat{\rho}_+ - \hat{\rho}_-} - 1) + \rho_+ (e^{-\hat{\rho}_+ + \hat{\rho}_-} - 1)
\end{aligned} \tag{S-26b}$$

where  $\mathcal{E} = \ell_e^2 / \ell_d^2 \in [0, 1]$  is a measure of the relative exchange rate.

We can write the above path integral description in terms of the total density and polarisation fields and include only the terms which are at most quadratic in the corresponding response fields only. This gives

$$\text{Pr} [\rho(x, t_{\text{fin}}), m(x, t_{\text{fin}}) | \rho(x, t_{\text{ini}}), m(x, t_{\text{ini}})] \simeq \int [\mathcal{D}\rho] [\mathcal{D}m] [\mathcal{D}\hat{\rho}] [\mathcal{D}\hat{m}] e^{-\ell_d \int dt \int dx (\hat{\rho} \partial_t \rho + \hat{m} \partial_t m) - H[\rho, m, \hat{\rho}, \hat{m}]} \tag{S-27a}$$

with the Hamiltonian

$$\begin{aligned}
H = \int dx & \left\{ \rho (1 - \rho) (\partial_x \hat{\rho})^2 + [\rho (1 - \rho + \mathcal{E} \rho) - \mathcal{E} m^2] (\partial_x \hat{m})^2 + 2 m (1 - \rho) \partial_x \hat{\rho} \partial_x \hat{m} \right. \\
& - [\partial_x \rho - \text{Pe} m (1 - \rho)] \partial_x \hat{\rho} - [(1 - \rho + \mathcal{E} \rho) \partial_x m + (m - \mathcal{E} m) \partial_x \rho - \text{Pe} \rho (1 - \rho)] \partial_x \hat{m} \\
& \left. + 2 \rho \hat{m}^2 - 2 m \hat{m} \right\}
\end{aligned} \tag{S-27b}$$

The fluctuating hydrodynamic equations are then given as

$$\partial_t \rho = \partial_x^2 \rho - \text{Pe} \partial_x [m (1 - \rho)] + \frac{1}{\sqrt{\ell_d}} \partial_x \eta_\rho \tag{S-28a}$$

$$\partial_t m = (1 - \rho + \mathcal{E} \rho) \partial_x^2 m + (m - \mathcal{E} m) \partial_x^2 \rho - \text{Pe} \partial_x [\rho (1 - \rho)] - 2m + \frac{1}{\sqrt{\ell_d}} (\partial_x \eta_m + 2 \eta_f) \tag{S-28b}$$

where the Gaussian noises  $\eta_\rho$ ,  $\eta_m$  and  $\eta_f$  have zero mean and covariances

$$\langle \eta_\rho(x, t) \eta_\rho(x', t') \rangle = 2 \rho (1 - \rho) \delta(x - x') \delta(t - t') \tag{S-28c}$$

$$\langle \eta_m(x, t) \eta_m(x', t') \rangle = 2 [\rho (1 - \rho + \mathcal{E} \rho) - \mathcal{E} m^2] \delta(x - x') \delta(t - t') \tag{S-28d}$$

$$\langle \eta_f(x, t) \eta_f(x', t') \rangle = \rho \delta(x - x') \delta(t - t') \tag{S-28e}$$

$$\langle \eta_\rho(x, t) \eta_m(x', t') \rangle = 2 m (1 - \rho) \delta(x - x') \delta(t - t') \tag{S-28f}$$

$$\langle \eta_\rho(x, t) \eta_f(x', t') \rangle = \langle \eta_m(x, t) \eta_f(x', t') \rangle = 0 \tag{S-28g}$$

The case of  $\mathcal{E} = 1$  corresponds to an arguably unphysical scenario where a particle moves to an adjacent occupied site by exchanging its position with the occupant at a rate which is exactly equal to the rate at which the particle would have moved to the site had it been empty. This is the model whose noiseless hydrodynamics was studied in [2] and subsequently the fluctuating hydrodynamic description was studied in [3]. We recover the fluctuating hydrodynamic description for our model by taking  $\mathcal{E} = 0$  as expected.

#### S-4. THE SPINODAL ANALYSIS

The noiseless hydrodynamics is obtained from (S-17) by setting the noise terms equal to zero

$$\partial_t \rho = -\partial_x \bar{J}_\rho \tag{S-29a}$$

$$\partial_t m = -\partial_x \bar{J}_m - 2 \bar{J}_f \tag{S-29b}$$

where the conservative currents  $\bar{J}_\rho$  and  $\bar{J}_m$  arising due to biased-diffusion dynamics are given in (S-16e) and (S-16f) respectively while the non-conservative current  $\bar{J}_f$  arising due to tumbling events is given in (S-16g).

A particular solution for the stationary state of (S-29) is given by the homogeneous profiles  $\rho(x, t) = \rho_0$  and  $m(x, t) = 0$ . We perturb the stationary homogeneous profiles as  $\rho(x, t) = \rho_0 + \delta\rho(x, t)$  and  $m(x, t) = \delta m(x, t)$  with  $\delta\rho$

and  $\delta m$  being small fluctuations in the hydrodynamic fields. This allows us to write the hydrodynamics for the small perturbations up to the leading order as

$$\partial_t(\delta\rho) = \partial_x^2(\delta\rho) - \text{Pe}(1 - \rho_0)\partial_x(\delta m) \quad (\text{S-30a})$$

$$\partial_t(\delta m) = (1 - \rho_0)\partial_x^2(\delta m) - \text{Pe}(1 - 2\rho_0)\partial_x(\delta\rho) - 2\delta m \quad (\text{S-30b})$$

Defining the continuous Fourier-transformation

$$\begin{pmatrix} \tilde{\delta\rho}(k, t) \\ \tilde{\delta m}(k, t) \end{pmatrix} = \frac{1}{L/\ell_d} \int_0^{L/\ell_d} dx e^{-ikx} \begin{pmatrix} \delta\rho(x, t) \\ \delta m(x, t) \end{pmatrix} \quad (\text{S-31})$$

for a large  $L/\ell_d$ , we can rewrite the Fourier-transformed noiseless hydrodynamic equations for the small fluctuating fields as

$$\partial_t \begin{pmatrix} \tilde{\delta\rho}(k, t) \\ \tilde{\delta m}(k, t) \end{pmatrix} = \begin{pmatrix} -k^2 & -i\text{Pe}(1 - \rho_0)k \\ i\text{Pe}(2\rho_0 - 1)k & -(1 - \rho_0)k^2 - 2 \end{pmatrix} \begin{pmatrix} \tilde{\delta\rho}(k, t) \\ \tilde{\delta m}(k, t) \end{pmatrix} \quad (\text{S-32})$$

where  $k = 2\pi n\ell_d/L$  with  $n = 0, \pm 1, \pm 2, \dots$ . The eigenvalues of the above matrix are given by

$$\lambda_{\pm}(k) = -1 - \left(1 - \frac{\rho_0}{2}\right)k^2 \pm \sqrt{1 + [\text{Pe}^2(1 - \rho_0)(2\rho_0 - 1) - \rho_0]k^2 + \frac{\rho_0^2 k^4}{4}} \quad (\text{S-33})$$

which obey the symmetry  $\lambda_{\pm}(-k) = \lambda_{\pm}(k)$ .

The two eigenvalues  $\lambda_+(0) = 0$  and  $\lambda_-(0) = -2$  corresponding to the  $k = 0$  mode respectively describe the invariance of the spatially integrated total density  $\int dx \rho(x, t)$  and the exponential decay of the spatially integrated polarisation  $M(t) = \int dx m(x, t) = M(0)e^{-2t}$ , which also directly follows from S-29.

The homogeneous solutions become linearly unstable at large wavelengths when one of the eigenvalues corresponding to the first mode (i.e.,  $k = \pm 2\pi/(L/\ell_d)$ ) becomes positive,  $\lambda_+(2\pi/(L/\ell_d)) > 0$ . This, consequently, puts a condition on the macroscopic size of the system as

$$L/\ell_d > \frac{2\pi\sqrt{1 - \rho_0}}{\sqrt{\text{Pe}^2(1 - \rho_0)(2\rho_0 - 1) - 2}} \quad (\text{S-34})$$

Note that the term within the square root in the denominator must be positive, i.e.,

$$\text{Pe}^2(1 - \rho_0)(2\rho_0 - 1) > 2 \quad (\text{S-35})$$

Interestingly, this is the same instability condition found earlier [2], where the single-file constraint is not respected and a  $\pm$  pair of particles at neighboring sites is allowed to exchange their positions at a rate  $\ell_d^2/\tau_p$ . The above condition is equivalent to

$$(\rho_0 - \rho_l^s)(\rho_0 - \rho_h^s) < 0 \quad (\text{S-36})$$

where

$$\rho_l^s = \frac{3}{4} - \frac{1}{4}\sqrt{1 - \left(\frac{4}{\text{Pe}}\right)^2} \quad \text{and} \quad \rho_h^s = \frac{3}{4} + \frac{1}{4}\sqrt{1 - \left(\frac{4}{\text{Pe}}\right)^2} \quad (\text{S-37})$$

Therefore, for  $\text{Pe} > 4$ , the system is linearly unstable in the spinodal region given by  $\rho_0 \in [\rho_l^s, \rho_h^s]$ .

## S-5. THE BINODAL ANALYSIS

For a system in a phase-separated state, a high density liquid-like phase and a low density gas-like phase coexist. The binodal or the coexistence curve gives the two densities, denoted by  $\rho_l$  and  $\rho_g$  respectively, as a function of a control parameter, which in our case is the Péclet number  $\text{Pe}$ . To compute the binodal, we use the procedure followed in [2, 4], which we outline below for the convenience of the readers.

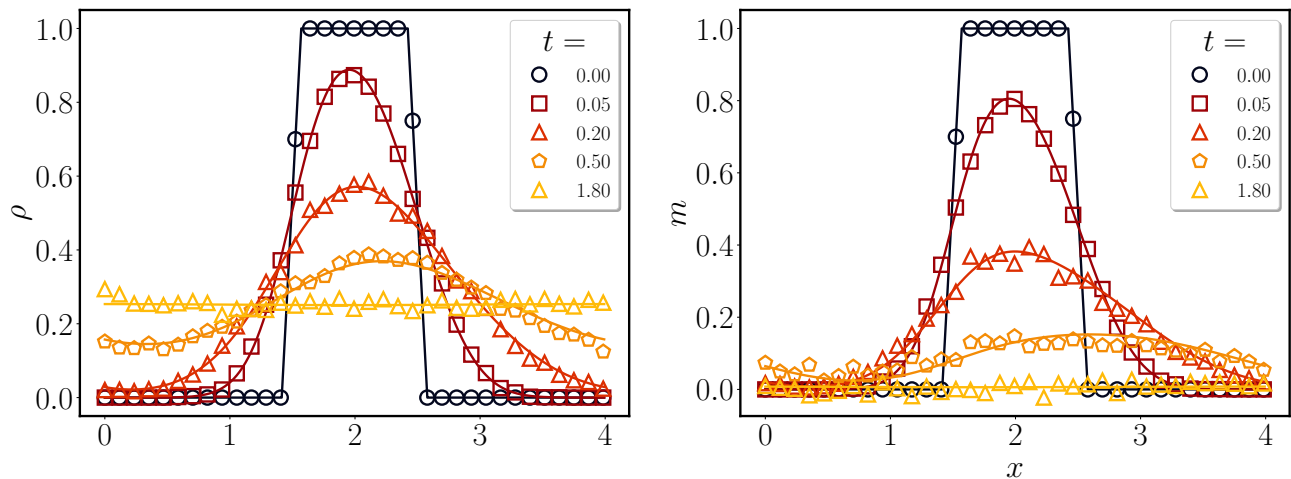


FIG. S-1. **Validity of hydrodynamics for quasi-1D model:** These plots demonstrate the agreement between microscopics and hydrodynamics outside the spinodal region (S-36). Time evolution of the hydrodynamic density  $\rho(x,t)$  and polarisation  $m(x,t)$ , starting from a step profile for both  $\rho(x,0)$  and  $m(x,0)$  centered around the middle of the system. The solid lines represent noiseless hydrodynamics evolution (S-17), while the markers represent Monte-Carlo simulations of the microscopic dynamics for the two-lane ladder-lattice model. The plots are for microscopic parameter values  $\ell_d = 128$ ,  $\tau_p = \ell_d^2$ ,  $\ell_p = 2\ell_d$ ,  $\tau_x = 0.05$  and system size  $L = 4\ell_d$  which corresponds to  $Pe = 2$ . To match with noiseless hydrodynamics, the Monte-Carlo results are averaged over 64 realisations. The hydrodynamic simulations are performed in the domain  $[0, L/\ell_d = 4]$  using pseudospectral method with  $2^9$  modes.

The stationary state is given by  $\partial_t \rho = 0$ , which has a zero flux due to symmetry, which gives us  $\bar{J}_\rho = 0$ . Using (S-16e), we obtain

$$m = \frac{1}{Pe} \frac{\partial_x \rho}{1 - \rho} = -\frac{1}{Pe} \partial_x [\log(1 - \rho)] \quad (\text{S-38})$$

The stationary state for the polarization field i.e.,  $\partial_t m = 0$  gives us  $\partial_x \bar{J}_m - 2\bar{J}_f = 0$ , which, using (S-16f), (S-16g) and the above expression of  $m$ , can be rewritten as

$$\partial_x g = 0 \quad \text{where} \quad g(\rho) = g_0(\rho) + \Lambda(\rho) (\partial_x \rho)^2 - \kappa \partial_x^2 \rho = \text{const.} \quad (\text{S-39})$$

$$\text{with} \quad g_0(\rho) = Pe \rho(1 - \rho) - \frac{2}{Pe} \log(1 - \rho), \quad \Lambda(\rho) = -\frac{2}{Pe} \frac{1}{1 - \rho} \quad \text{and} \quad \kappa = \frac{1}{Pe} \quad (\text{S-40})$$

The spinodal curve is equivalently defined by  $g'_0(\rho) = 0$ , whose two solutions are given by  $\rho_l^s$  and  $\rho_h^s$  respectively (see (S-37)).

### A. First relation

In the coexisting phase, density is homogeneous in the liquid ( $\rho_l$ ) and gas ( $\rho_g$ ) phases:  $\partial_x \rho = \partial_x^2 \rho = 0$  in the two phases, giving

$$g_0(\rho_g) = g_0(\rho_l) \equiv \bar{g}(Pe) \quad (\text{S-41})$$

For  $Pe < 4$ ,  $g_0(\rho)$  is a monotonic function of  $\rho$ . On the other hand, it has a maximum and minimum at  $\rho_l^s$  and  $\rho_h^s$  respectively for  $Pe > 4$  [see Fig. S-2]. For  $Pe = 4$ , there is an inflection point at  $\rho = 3/4$ , where both  $g'_0(\rho)$  and  $g''_0(\rho)$  are zero. For  $Pe > 4$ , any line  $g_0(\rho) = \text{const.} \in (g_0(\rho_l^s), g_0(\rho_h^s))$ , intersects the  $g_0(\rho)$  vs.  $\rho$  curve at three points, and therefore, there exists an infinite number of solutions for (S-41). Hence, we need another relation for fixing the coexistence densities, which we discuss below.



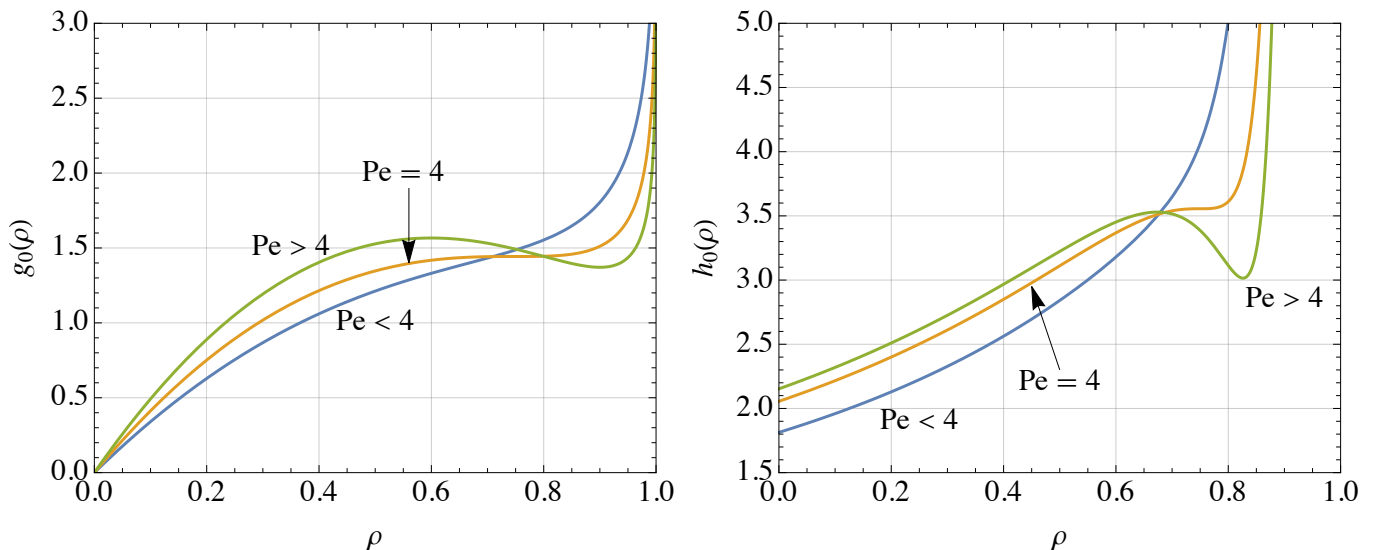


FIG. S-2. The binodal curves are given by the pair of conditions  $g_0(\rho_g) = g_0(\rho_l)$  and  $h_0(\rho_g) = h_0(\rho_l)$ , where the expressions of  $g_0(\rho)$  and  $h_0(\rho)$  are given by (S-40) and (S-52) respectively. Here,  $g_0(\rho)$  and  $h_0(\rho)$  are plotted as a function of  $\rho$  on the left and right figures, respectively. For  $Pe < 4$ , both they are monotonic functions of  $\rho$ . On the other hand, for  $Pe$ , both  $g_0(\rho)$  and  $h_0(\rho)$  have a minimum and a maximum. For  $Pe = 4$ , there is an inflection point at  $\rho = 3/4$ , where the first and the second derivatives of both  $g_0$  and  $h_0$  vanish.

### B. Second relation

Consider the following integral across the liquid-gas interface in a phase-separated state

$$I = \int_{x_g}^{x_l} dx g(\rho) \partial_x R(\rho) \quad (\text{S-42})$$

where  $R(\rho)$  is some function of  $\rho$ , and  $x_g$  and  $x_l$  are any two points inside the gas and liquid phases respectively. Since,  $g(\rho) = \bar{g}$  is constant, the above integral yields

$$I = \bar{g} [R(\rho_l) - R(\rho_g)] \quad (\text{S-43})$$

On the other hand, substituting the expression of  $g(\rho)$  from (S-39) in the integral gives

$$I = \int_{x_g}^{x_l} dx g_0(\rho) \partial_x R(\rho) + \int_{x_g}^{x_l} dx [\Lambda(\rho) R'(\rho) (\partial_x \rho)^2 - \kappa R'(\rho) \partial_x^2 \rho] \partial_x \rho \quad (\text{S-44})$$

Now we choose  $R(\rho)$  such that the second integral is zero. Consider the relation

$$\partial_x [A(\rho) (\partial_x \rho)^2] = [A'(\rho) (\partial_x \rho)^2 + 2A(\rho) \partial_x^2 \rho] \partial_x \rho \quad (\text{S-45})$$

Choosing,  $2A(\rho) = -\kappa R'(\rho)$  and  $\kappa R''(\rho) = -2\Lambda(\rho) R'(\rho)$ , the above relation gives

$$[\Lambda(\rho) R'(\rho) (\partial_x \rho)^2 - \kappa R'(\rho) \partial_x^2 \rho] \partial_x \rho = -\partial_x \left[ \frac{\kappa}{2} R'(\rho) (\partial_x \rho)^2 \right] \quad (\text{S-46})$$

Since,  $\partial_x \rho = 0$  in the liquid and the gas phases, the integral over the above expression across the interface is zero. Hence, defining  $g_0(\rho) = d\phi(R)/dR$ , from (S-44) we get

$$I = \phi(R_l) - \phi(R_g) \quad (\text{S-47})$$

where  $R_l = R(\rho_l)$  and  $R_g = R(\rho_g)$ . Combining the two expressions of  $I$ , (S-43) and (S-47), we arrive at the relation

$$h_0(R_g) = h_0(R_l) \quad \text{where} \quad h_0(R) = R\phi'(R) - \phi(R) \quad (\text{S-48})$$

For the particular form of  $\Lambda(\rho)$  given above, the above differential equation of  $R(\rho)$  can be solved exactly to give (up to an additive and a multiplicative constant)

$$R(\rho) = \frac{1}{3} \frac{1}{(1-\rho)^3} \quad (\text{S-49})$$

Inverting the above equation, we can express  $\rho(R) = 1 - (3R)^{-1/3}$ , which in turn gives

$$\phi'(R) = \text{Pe}[1 - (3R)^{-1/3}](3R)^{-1/3} + \frac{2}{3\text{Pe}} \log(3R) \quad (\text{S-50})$$

Now, integrating with respect to  $R$  gives (up to an additive constant, which doesn't show up in the relation)

$$\phi(R) = \text{Pe} \left[ \frac{(3R)^{1/3}}{2} - 1 \right] (3R)^{1/3} + \frac{2R}{3\text{Pe}} [\log(3R) - 1] \quad (\text{S-51})$$

Therefore,  $h_0(R(\rho))$  can be expressed in terms of  $\rho$  explicitly as

$$h_0(\rho) = \frac{2}{9\text{Pe}} \frac{1}{(1-\rho)^3} + \frac{\text{Pe}}{6} \frac{3-4\rho}{(1-\rho)^2} \quad (\text{S-52})$$

and the second coexistence relation can now be written as

$$h_0(\rho_g) = h_0(\rho_l). \quad (\text{S-53})$$

The qualitative behavior of  $h_0$  is similar to that of  $g_0(\rho)$  [see Fig. S-2]. For  $\text{Pe} < 4$ ,  $h_0(\rho)$  is a monotonic function of  $\rho$ , whereas for  $\text{Pe} > 4$ , it has a maximum and a minimum at  $\rho_l^s$  and  $\rho_h^s$  respectively. For  $\text{Pe} = 4$ , there is an inflection point at  $\rho = 3/4$ , where both  $h_0'(\rho)$  and  $h_0''(\rho)$  are zero.

Interestingly, the two solutions of  $h_0'(\rho) = 0$  are same as that of  $g_0'(\rho) = 0$  and are given by  $\rho_l^s$  and  $\rho_h^s$  respectively [see (S-37)]. This follows from using  $\phi'(R) = g_0(\rho)$ , writing  $h_0(\rho) = R(\rho)g_0(\rho) - \phi(R(\rho))$  and taking a derivative with respect to  $\rho$

$$h_0'(\rho) = R(\rho) g_0'(\rho) + R'(\rho) g_0(\rho) - R'(\rho) \phi'(R) = R(\rho) g_0'(\rho) \quad (\text{S-54})$$

The binodal curves are obtained by numerically solving the relations  $g_0(\rho_g) = g_0(\rho_l)$  and  $h_0(\rho_g) = h_0(\rho_l)$ , where the expressions of  $g_0(\rho)$  and  $h_0(\rho)$  are given by (S-40) and (S-52) respectively.

## S-6. THE TWO-POINT CORRELATIONS IN THE STATIONARY-STATE HOMOGENEOUS PHASE

In this Section, we present the derivation of the two-point correlations of the hydrodynamic fields in the stationary state of the homogeneous phase of our model. This serves as an indirect check of our fluctuating hydrodynamic description as reported in eq. (1) of the *Letter*. Our result for the correlations is valid up to the leading order in  $1/\ell_d$  and for this purpose, we use only the Gaussian noise approximation ignoring any sub-leading terms.

We begin our derivation by adding small fluctuations,  $\delta\rho(x, t)$  and  $\delta m(x, t)$  which are of at most  $\mathcal{O}(1/\sqrt{\ell_d})$  around the stationary-state homogeneous fields,  $\rho(x, t) = \rho_0$  and  $m(x, t) = 0$  respectively. The definition of the two-point correlations of the fluctuating fields [5] then readily follows

$$C_{\rho\rho}(x, x') = \langle \delta\rho(x, t) \delta\rho(x', t) \rangle, \quad C_{\rho m}(x, x') = \langle \delta\rho(x, t) \delta m(x', t) \rangle \quad \text{and} \quad C_{mm}(x, x') = \langle \delta m(x, t) \delta m(x', t) \rangle. \quad (\text{S-55})$$

Putting these perturbed total density and polarisation fields in eq. (1) of the *Letter* and keeping only the terms which are at most linear in  $\delta\rho$  and  $\delta m$ , we obtain the fluctuating hydrodynamic equations

$$\partial_t \begin{pmatrix} \delta\rho(x, t) \\ \delta m(x, t) \end{pmatrix} = \mathbf{D}_x \begin{pmatrix} \delta\rho(x, t) \\ \delta m(x, t) \end{pmatrix} + \mathbf{F}(x, t) \quad (\text{S-56a})$$

with the deterministic,  $\mathbf{D}_x$  and fluctuating,  $\mathbf{F}(x, t)$  components are respectively given as

$$\mathbf{D}_x = \begin{pmatrix} \partial_x^2 & -\text{Pe}(1-\rho_0)\partial_x \\ -\text{Pe}(1-2\rho_0)\partial_x & (1-\rho_0)\partial_x^2 - 2 \end{pmatrix} \quad \text{and} \quad \mathbf{F}(x, t) = \sqrt{\frac{2\rho_0}{\ell_d}} \begin{pmatrix} \sqrt{1-\rho_0}\partial_x\eta_\rho \\ \sqrt{1-\rho_0}\partial_x\eta_m + \sqrt{2}\eta_f \end{pmatrix} \quad (\text{S-56b})$$

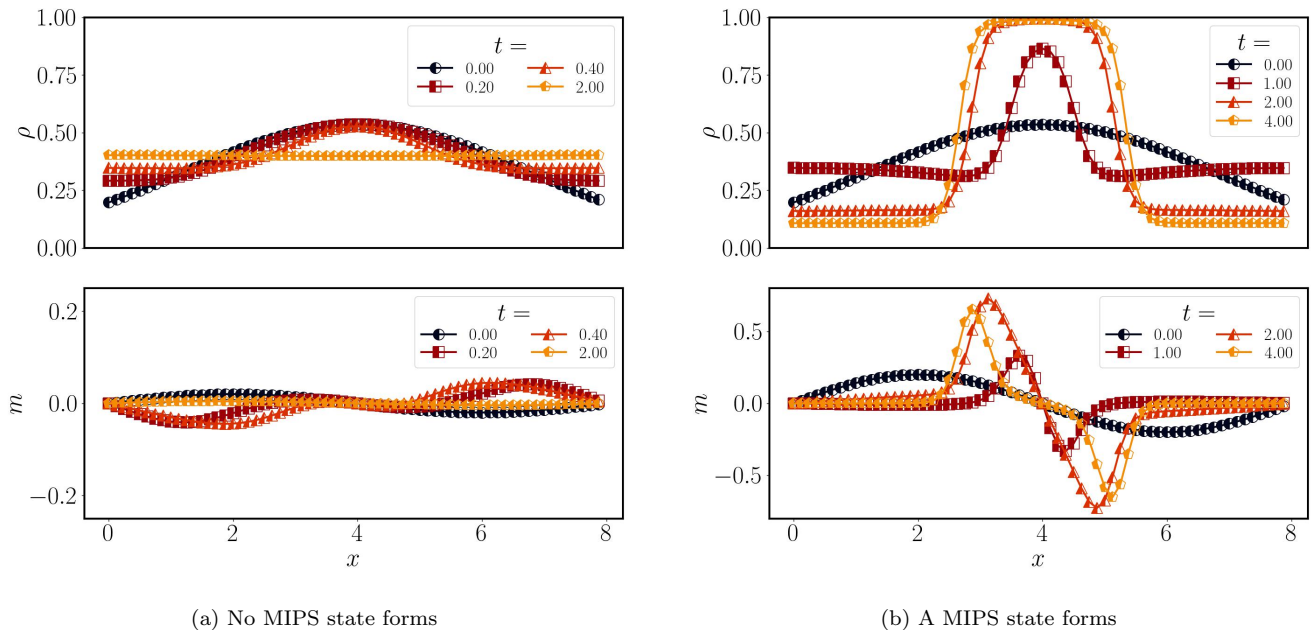


FIG. S-3. **Metastability:** Here, we demonstrate that although the region outside the spinodal curve but inside the binodal curve is linearly stable, depending on the initial state there are nonlinear instabilities which may drive the system to MIPS. We have set  $Pe = 10$  and  $\rho_0 = 0.4$  for making these plots which corresponds to a point between the spinodal and binodal curves. We have taken an identical Gaussian initial total density profile, but for the initial polarisation profile, we have taken  $\sin 2\pi x/L$  with amplitude 0.02 for the left figure and 0.2 for the right figure.

where  $\eta_\rho(x, t)$ ,  $\eta_m(x, t)$  and  $\eta_f(x, t)$  are delta-correlated Gaussian white noises with unit self-covariance and zero cross-covariance.

In the large hydrodynamic system size limit  $L/\ell_d \rightarrow \infty$ , we define the continuous-Fourier-transformed fluctuating hydrodynamic fields as

$$\begin{pmatrix} \delta\tilde{\rho}(k, t) \\ \delta\tilde{m}(k, t) \end{pmatrix} = \frac{1}{2\pi} \int_{-\infty}^{\infty} dx \begin{pmatrix} \delta\rho(x, t) \\ \delta m(x, t) \end{pmatrix} e^{-ikx} \quad (\text{S-57})$$

and subsequently re-write the fluctuating hydrodynamic equations in the Fourier space

$$\partial_t \begin{pmatrix} \delta\tilde{\rho}(k, t) \\ \delta\tilde{m}(k, t) \end{pmatrix} = \tilde{\mathbf{D}}_k \begin{pmatrix} \delta\tilde{\rho}(k, t) \\ \delta\tilde{m}(k, t) \end{pmatrix} + \tilde{\mathbf{F}}(k, t) \quad (\text{S-58a})$$

with the deterministic and fluctuating components in the Fourier space respectively given by

$$\tilde{\mathbf{D}}_k = \begin{pmatrix} -k^2 & -iPe(1-\rho_0)k \\ -iPe(1-2\rho_0)k & -(1-\rho_0)k^2 - 2 \end{pmatrix} \quad \text{and} \quad \tilde{\mathbf{F}}(k, t) = \sqrt{\frac{2\rho_0}{\ell_d}} \begin{pmatrix} i\sqrt{1-\rho_0}k\tilde{\eta}_1(k, t) \\ \sqrt{(1-\rho_0)k^2 + 2}\tilde{\eta}_2(k, t) \end{pmatrix} \quad (\text{S-58b})$$

where  $\tilde{\eta}_1(k, t)$  and  $\tilde{\eta}_2(k, t)$  are Gaussian noises with mean and covariance

$$\langle \eta_\alpha(x, t) \rangle = 0 \quad \text{and} \quad \langle \eta_\alpha(x, t) \eta_{\alpha'}(x', t') \rangle = \delta_{\alpha, \alpha'} \delta(x - x') \delta(t - t') \quad \text{where } \alpha, \alpha' = \{1, 2\}. \quad (\text{S-58c})$$

The differential equations in (S-58a) can now be readily solved that leads to the solutions of the fluctuation fields in Fourier space in terms of  $\tilde{\mathbf{D}}_k$  and  $\tilde{\mathbf{F}}(k, t)$  as

$$\begin{pmatrix} \delta\tilde{\rho}(k, t) \\ \delta\tilde{m}(k, t) \end{pmatrix} = \int_{-\infty}^t dt' e^{\mathbf{D}_k(t-t')} \mathbf{F}(k, t') \quad (\text{S-59})$$

The two-point correlations of the fluctuating hydrodynamic fields in the Fourier space is then obtained using the Fourier-transformed definitions of (S-55) which are given by  $C_{\rho\rho}(k, k') = \langle \delta\rho(k, t) \delta\rho(k', t) \rangle$ ,  $C_{mm}(k, k') =$

$\langle \delta m(k, t) \delta m(k', t) \rangle$  and  $C_{\rho m}(k, k') = \langle \delta \rho(k, t) \delta m(k', t) \rangle$ . For instance, the correlations between the total density fields of two points in Fourier space is given by

$$\tilde{C}_{\rho\rho}(k, k') = \frac{\rho_0 (1 - \rho_0) \left\{ (1 - \rho_0) (2 - \rho_0) k^4 + [4(1 - \rho_0) + \text{Pe}^2 (1 - \rho_0)^2 + \chi^2] k^2 + 2 [2 + \text{Pe}^2 (1 - \rho_0)] \right\}}{\left\{ (1 - \rho_0) (2 - \rho_0) k^4 + [2(1 - \rho_0) + (2 - \rho_0) \chi^2] k^2 + 2 \chi^2 \right\} \ell_d} \delta(k + k') \quad (\text{S-60})$$

where the parameter

$$\chi = \sqrt{2 - \text{Pe}^2 (1 - \rho_0) (2\rho_0 - 1)} \quad (\text{S-61})$$

determines the onset of linear instability of the stationary-state homogeneous fields under small perturbations i.e., the spinodal region.

The  $k = (k' =) 0$  mode relates to the spatial integral of the fluctuations of the total density field,  $\int dx \delta \rho(x, t)$ . Although the total number of particles in the two-lane system as a whole is conserved, the number of particles in each of the lanes is allowed to fluctuate due to the lane-crossing dynamics. This particle number fluctuation in the two lanes of the system can be assumed to be independent of each other in the long time limit which implies that the  $2 \times \tilde{C}_{\rho\rho}(k, k')$  must vanish when  $k = (k' =) 0$ . We take this into account by including an additional  $k = (k' =) 0$  term proportional to the infinitesimal inter-mode width  $\ell_d/L$ , such that the correlation in (S-60) is now given as

$$\tilde{C}_{\rho\rho}(k, k') = \left[ \frac{\rho_0 (1 - \rho_0) \left\{ (1 - \rho_0) (2 - \rho_0) k^4 + [4(1 - \rho_0) + \text{Pe}^2 (1 - \rho_0)^2 + \chi^2] k^2 + 2 [2 + \text{Pe}^2 (1 - \rho_0)] \right\}}{\left\{ (1 - \rho_0) (2 - \rho_0) k^4 + [2(1 - \rho_0) + (2 - \rho_0) \chi^2] k^2 + 2 \chi^2 \right\} \ell_d} - \frac{\rho_0 (1 - \rho_0) [2 + \text{Pe}^2 (1 - \rho_0)]}{2 \chi^2 L} \delta(k) \right] \delta(k + k') \quad (\text{S-62})$$

Similarly, the correlations of total density with polarisation and polarisation with polarisation are respectively given as

$$\tilde{C}_{\rho m}(k, k') = \frac{-2i \text{Pe} \rho_0^2 (1 - \rho_0) [(1 - \rho_0) k^2 + 2] k}{\left\{ (1 - \rho_0) (2 - \rho_0) k^4 + [2(1 - \rho_0) + (2 - \rho_0) \chi^2] k^2 + 2 \chi^2 \right\} \ell_d} \delta(k + k') \quad (\text{S-63})$$

$$\tilde{C}_{mm}(k, k') = \frac{\rho_0 \left\{ (1 - \rho_0) (2 - \rho_0) k^4 + [2(2 - \rho_0) + \text{Pe}^2 (1 - \rho_0) (1 - 2\rho_0)^2 + (1 - \rho_0) \chi^2] k^2 + 2 \chi^2 \right\}}{\left\{ (1 - \rho_0) (2 - \rho_0) k^4 + [2(1 - \rho_0) + (2 - \rho_0) \chi^2] k^2 + 2 \chi^2 \right\} \ell_d} \delta(k + k') \quad (\text{S-64})$$

In the above two expression of the correlations involving the polarisation fields, we do not have any additional  $k = (k' =) 0$  term, as the spatially-integrated fluctuating polarisation fields  $\int dx \delta m(x, t)$  do not vanish.

Finally, we take the inverse Fourier transformation of the expressions in (S-62-S-63), which gives the two-point correlations for the fluctuating hydrodynamic fields in the stationary-state homogeneous phase. These are respectively given by

$$C_{\rho\rho}(x, x') = \frac{\text{Pe}^2 \rho_0^2 (1 - \rho_0)^2}{[2 - \text{Pe}^2 (1 - \rho_0) (2 - \rho_0) (2\rho_0 - 1)] \ell_d} \left[ \sqrt{\frac{2}{2 - \rho_0}} e^{-\frac{|x-x'|}{\xi_1}} + \sqrt{1 - \rho_0} \frac{\chi^2 - 2}{\chi} e^{-\frac{|x-x'|}{\xi_2}} \right] + \frac{\rho_0 (1 - \rho_0)}{\ell_d} \delta(x - x') - \frac{\rho_0 (1 - \rho_0) [2 + \text{Pe}^2 (1 - \rho_0)]}{2 \chi^2 L} \quad (\text{S-65a})$$

$$C_{\rho m}(x, x') = \text{sgn}(x - x') \frac{\text{Pe} \rho_0^2 (1 - \rho_0)}{[2 - \text{Pe}^2 (1 - \rho_0) (2 - \rho_0) (2\rho_0 - 1)] \ell_d} \left[ \frac{2}{2 - \rho_0} e^{-\frac{|x-x'|}{\xi_1}} + (\chi^2 - 2) e^{-\frac{|x-x'|}{\xi_2}} \right] \quad (\text{S-65b})$$

$$C_{mm}(x, x') = \frac{\text{Pe}^2 \rho_0^2 (1 - \rho_0) (1 - 2\rho_0)}{[2 - \text{Pe}^2 (1 - \rho_0) (2 - \rho_0) (2\rho_0 - 1)] \ell_d} \left( \sqrt{\frac{2}{2 - \rho_0}} e^{-\frac{|x-x'|}{\xi_1}} - \frac{\chi}{\sqrt{1 - \rho_0}} e^{-\frac{|x-x'|}{\xi_2}} \right) + \frac{\rho_0}{\ell_d} \delta(x - x') \quad (\text{S-65c})$$

where the two ‘‘correlation lengths’’ corresponding to the length scales of the exponentially decaying long-range correlations are

$$\xi_1 = \sqrt{1 - \frac{\rho_0}{2}} \quad \text{and} \quad \xi_2 = \frac{\sqrt{1 - \rho_0}}{\chi} \quad (\text{S-66})$$



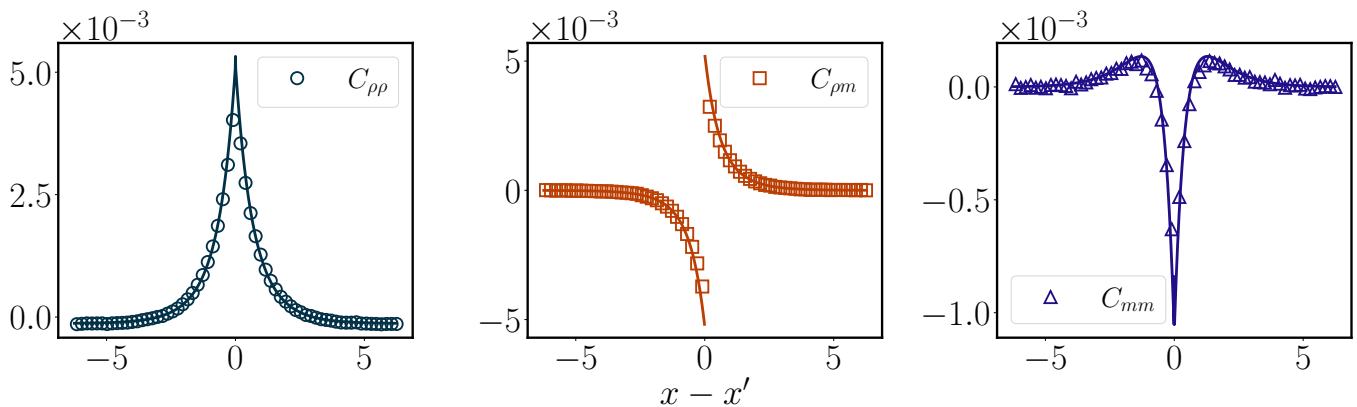


FIG. S-4. **Two-point correlations in stationary-state homogeneous phase:** We find excellent agreement between the hydrodynamic predictions of the two point correlations (S-65) and the Monte-Carlo simulations. For the Monte-Carlo simulations, we define the correlations  $C_{\rho\rho}(i, i') = \langle n_i n_{i'} \rangle - \langle n_i \rangle \langle n_{i'} \rangle$ ,  $C_{\rho m}(i, i') = \langle n_i M_{i'} \rangle - \langle n_i \rangle \langle M_{i'} \rangle$  and  $C_{mm}(i, i') = \langle M_i M_{i'} \rangle - \langle M_i \rangle \langle M_{i'} \rangle$ , where,  $i$  and  $i'$  denotes the lattice sites,  $n_i = \{0, 1\}$  and  $M_i = \{0, \pm 1\}$  denotes the total occupation and polarisation of the  $i^{\text{th}}$  site, and  $\langle \cdot \rangle$  denotes the averaging over time. Additionally, due to translational symmetry in our system, spatial averaging is conducted to further refine the averaging. To compare with the fluctuating hydrodynamics results, we use the rescaling as  $x - x' = (i - i')/\ell_d$  discussed before. Evidently, the  $\rho$ - $\rho$  and  $m$ - $m$  correlations are symmetric in  $x - x'$  while the  $\rho$ - $m$  correlation is anti-symmetric in  $x - x'$ .

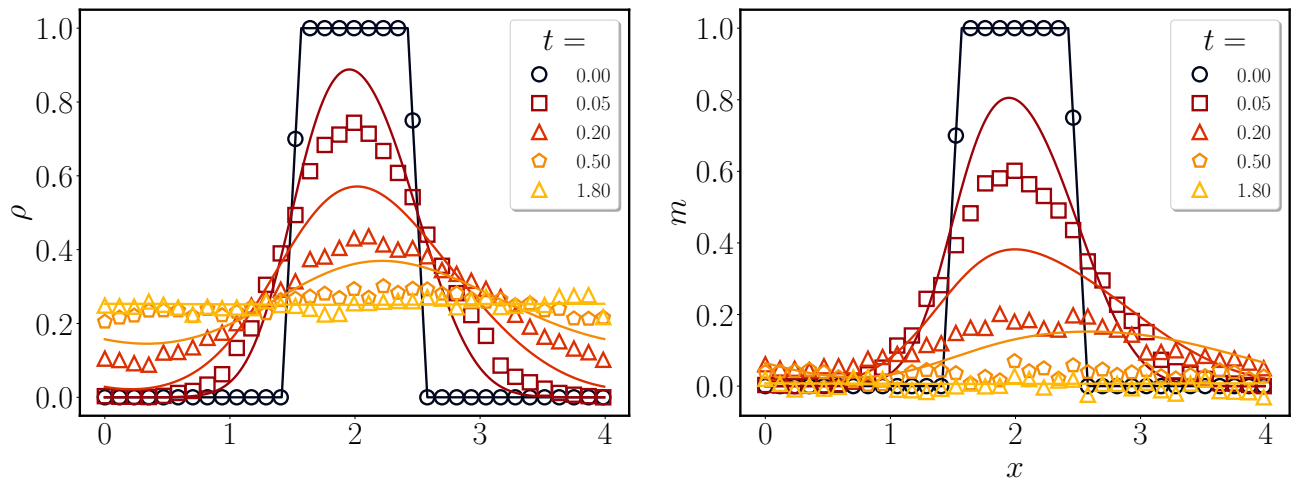


FIG. S-5. **Breakdown of noiseless hydrodynamics in strictly 1D:** Here, we show the breakdown of hydrodynamics in 1d even outside the Spinodal,  $\rho_0 = 0.25$ ,  $\text{Pe} = 2$ . We use the exact same initial condition and microscopic parameter values as Fig. S-1. We see that the hydrodynamics deviate quickly from the microscopics.

Two important observations are in order at this point. First, all the three correlations show a divergence when  $2 - \text{Pe}^2 (1 - \rho_0) (2 - \rho_0) (2\rho_0 - 1) \rightarrow 0$ . In fact, our results for the correlations are not valid in the region  $2 - \text{Pe}^2 (1 - \rho_0) (2 - \rho_0) (2\rho_0 - 1) \leq 0$ . Second,  $\xi_1 > \xi_2$  in the region  $2 - \text{Pe}^2 (1 - \rho_0) (2 - \rho_0) (2\rho_0 - 1) > 0$ . Consequently, the first exponential term in each of the correlations dominates over the second exponential term when the two points in space are far-separated i.e.,  $x - x' \gg 0$ .

Our results for the two-point correlations are reminiscent of the correlations arising in typical boundary-driven diffusive equilibrium systems [5] where the correlations consist of an equilibrium-like term which is delta-correlated in space and a long-range term whose strength decays with system size.

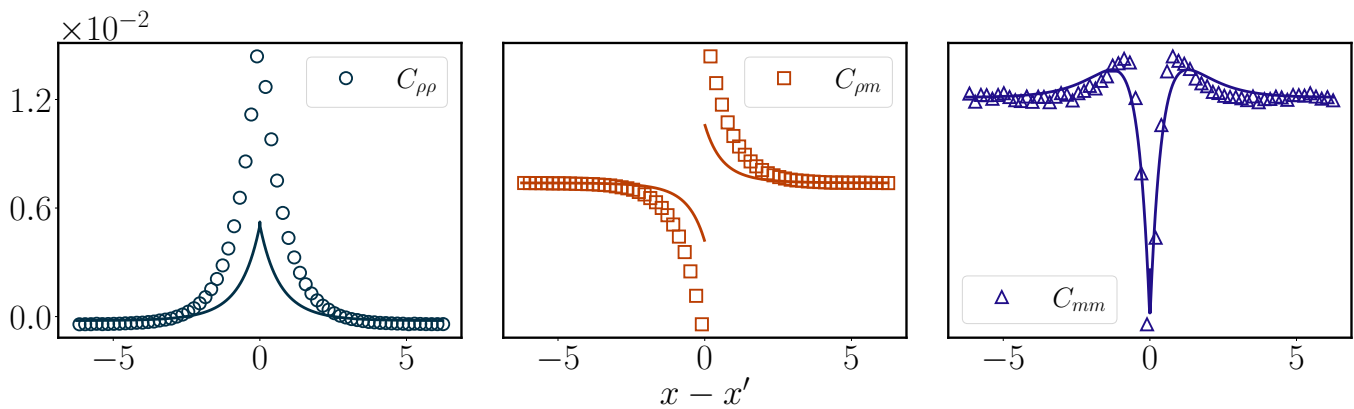


FIG. S-6. **Breakdown of fluctuating hydrodynamics in strictly 1D:** We perform Monte Carlo simulations outside the spinodal with  $\rho_0 = 0.25$ ,  $Pe = 2$  with exact same parameters in Fig. S-4 and find deviations from the predictions of the fluctuating hydrodynamics.

### S-7. DETAILS OF THE NUMERICAL SIMULATIONS

For the microscopic dynamics we use usual Monte Carlo method. We consider a periodic lattice with two lanes with  $L$  sites in each lane. We choose time step  $dt = 0.01$  to convert the rates to probability for the Monte Carlo simulations. The lane crossing rate  $1/\tau_x$  is taken as 10, 20 or 40 depending on the simulation.

To solve the hydrodynamic equations we employed the standard Fourier pseudospectral method [6], with nonlinear terms computed in real space using the  $\frac{2}{3}$  dealiasing rule [6]. Time integration was performed in Fourier space utilizing the standard Runge-Kutta 4th order (RK4) method and the Integrating Factor Runge-Kutta 4th order (IFRK4) method, with a time step ( $dt$ ) of  $10^{-3}$  or  $10^{-4}$ , depending on the system's resolution.

- 
- [1] S. Saha and T. Sadhu, Large deviations in the symmetric simple exclusion process with slow boundaries: A hydrodynamic perspective (2023), [arXiv:2310.11350v2](https://arxiv.org/abs/2310.11350v2) [[cond-mat.stat-mech](https://arxiv.org/abs/2310.11350v2)].
  - [2] M. Kourbane-Houssene, C. Erignoux, T. Bodineau, and J. Tailleur, Exact hydrodynamic description of active lattice gases, *Phys. Rev. Lett.* **120**, 268003 (2018).
  - [3] T. Agranov, S. Ro, Y. Kafri, and V. Lecomte, Exact fluctuating hydrodynamics of active lattice gases — typical fluctuations, *J. Stat. Mech.* **2021**, 083208 (2021).
  - [4] A. P. Solon, J. Stenhammar, M. E. Cates, Y. Kafri, and J. Tailleur, Generalized thermodynamics of phase equilibria in scalar active matter, *Phys. Rev. E* **97**, 020602(R) (2018).
  - [5] L. Bertini, A. De Sole, D. Gabrielli, G. Jona-Lasinio, and C. Landim, Towards a nonequilibrium thermodynamics: A self-contained macroscopic description of driven diffusive systems, *J. Stat. Phys.* **135**, 857–872 (2009).
  - [6] L. N. Trefethen, *Spectral methods in MATLAB* (SIAM Philadelphia, 2000).